# University of Alberta

On the Application of Effective Field Theory Methods to Polyelectrons

by

Paul Leslie McGrath

A thesis submitted to the Faculty of Graduate Studies and Research
in partial fulfillment of the requirements for the degree of

Master of Science

Department of Physics



Spring 2010
Edmonton, Alberta

## Examining Committee

Dr. Andrzej Czarnecki, Physics

Dr. Don Page, Physics

Dr. Alexander Penin, Physics

Dr. Alex Brown, Chemistry

**Abstract**

A recent study of the positronium atom showed that the energy levels could be determined numerically using an effective field theory just as easily as the underlying true theory. Here, we expand on this idea by modeling the three-body positronium-ion and four-body di-positronium molecule with low-energy effective field theories. We then compare the results obtained using the effective theories to those found in a similar manner with the true theory to determine if numerical calculations will converge more quickly using the effective field theory due to removal of the Coulomb divergence. Finally, with the necessary framework in place, we calculate a matrix element needed to evaluate the correction to the magnetic moment of the positronium-ion due to the interaction between the positron and the two electrons which form a spin singlet.

# Contents

## List of Tables

## List of Figures

# 1 Introduction

Many of our current theories of physics are most effectively applied perturbatively. For instance, in Quantum Electrodynamics (QED) one is often interested in calculating the probability for a particular event to occur. One way to do this is to consider all possible intermediate steps, or diagrams, that will result in this event and add them up. Each interaction in the intermediate steps decreases the order at which that diagram contributes to the total probability so only a finite number of diagrams need to be calculated to find the probability for a desired precision. One can increase the precision of their prediction from QED by calculating diagrams to higher and higher orders, in other words, by calculating more terms in the series.

Similar perturbative approaches are applied in extracting predictions from other physical theories as well. Unfortunately, as one moves to higher orders the interactions become more complicated and as a result the terms in the series become much more difficult to handle. In essence, as one moves to higher order processes they are dealing with terms that probe the dynamics of the system to higher energies or, equivalently, shorter distances. If one is only interested in exploring to high precision the low-energy behaviour of a system then using the full theory to calculate higher order corrections becomes extremely inefficient. This is when applying an effective field theory can be very useful.

In [18] Richard Hill constructs an effective field theory to determine the energy levels of the positronium atom. He argues that since the behaviour of positronium is dominated by low-energy interactions using the full theory of QED to determine the bound state energies is excessive. Using an effective field theory Hill shows that one can reproduce the results of the true theory to arbitrarily high precision. Positronium is an ideal candidate for using an effective field theory since it is a relatively low-energy system. However, the energy levels of the positronium atom with a purely Coulombic potential can be determined analytically and the higher order corrections due to relativistic and radiative effects have already been worked out to high precision [4]. The potential advantages of the effective field theory approach, in this case, may be somewhat hidden by being applied to such a well understood system. On the other hand, the dynamics of the positronium-ion and di-positronium molecule are also largely determined by the low-energy behaviour but cannot be solved analytically even when considering only Coulombic interactions. This makes both systems ideal testing grounds for moving to the next level and searching for possible advantages of using and effective field theory. Such an investigation is the focus of this work.

## 1.1 Polyelectrons

In 1928 Paul Dirac proposed that the bizarre negative energy solutions of his new wave equation for spin-half particles could be interpreted as antiparticles [10]. That is, his theory suggested that for every particle there exists a conjugate antiparticle with the same mass but opposite electric charge. In the simple case of the electron this meant that there should exist a particle with the same mass as the electron but with the charge of a proton. Indeed, in 1932 Carl D. Anderson confirmed the existence of the antielectron, or positron, by identifying it in a cloud chamber [2].

It turns out that after solving the wave equation for the bound states energies and wave functions of the hydrogen atom one finds that these solutions can be written

entirely in terms of the reduced mass of the system. This means that the stability of the system is not reliant upon the mass ratio of the proton and electron. This led Stjepan Mohorovičić to predict the existence of a hydrogen-like atom where a positron would replace the proton [29]. Later on, in 1951, Martin Deutsch would go on to discover this hydrogen-like atom composed of an electron and a positron and he would give it the name positronium which has stuck ever since [9].

However, even before the experimental discovery of positronium, the idea that positrons could be substituted for nuclei in more complex atoms and molecules had been investigated. In these cases the system would be composed of at least three particles which rendered finding an analytical solution impossible. Thus, the most appropriate method to see whether positrons could stabilize systems of three or more bodies was to use Ritz's variational principle.

John Wheeler presented the first proof that a system of two electrons and one positron - a positronium-ion - would form a stable state in 1946 [38]. Wheeler realized that the positronium-ion should be solvable using the methods previously applied to the Helium atom wherein the Helium atom was treated as a three-body system: one nucleus with twice the individual charge of two orbiting electrons. Following this reasoning Wheeler used essentially the same trial wave function that Egil Hylleraas used for the Helium atom and was able to show that it was more energetically favourable for the positronium-ion to form as compared to having a positronium atom and a free electron. In this calculation, Wheeler showed that the three-body system was stable against dissociation into a positronium atom and a free electron by an energy of at least 0.19 eV. In the same paper Wheeler went on to consider the four-body case of two electrons and two positrons, later dubbed di-positronium. He was able to show that the four-body entity was stable against dissociation into a positronium-ion and a free positron by an energy of at least 3 eV but was 3.6 eV shy of ruling out dissociation into two separate positronia atoms.

Aadne Ore and Egil Hylleraas picked up where Wheeler left off shortly thereafter. Ore performed his own variational calculation for di-positronium but was also unable to demonstrate that this state was stable although he was able to slightly close the gap of 3.6 eV that Wheeler had found to about 3.5 eV [30]. Hylleraas on the other hand worked on the positronium-ion and was able to increase the binding energy for a positronium atom and a free electron from 0.19 eV as found by Wheeler to over 0.20 eV [21]. Hylleraas and Ore would then combine their expertise later that year in a more sophisticated variational calculation to show that the four-body state, di-positronium, was in fact stable against dissociation into two positronia atoms by an energy of at least 0.11 eV thus providing the first proof that the di-positronium molecule should exist [22].

Extensive theoretical investigations of these polyelectron systems have continued to reveal their properties. The fundamentals of the positronium atom can be found in many textbooks [4] and higher order QED corrections have been laid out in a recent review by Penin [31]. Bhatia and Drachman [5], Frolov [13], Frost [16], and Ho [19], to name a few, have improved upon the predicted bound state energy of the positronium-ion. Likewise, the bound state energy of di-positronium has been determined to higher precision by Frolov [14], Ho [20], and Rebane [36] among others. Studies by Bubin et al. [8], Puchalski and Czarnecki [35, 34], and others have taken the next step by calculating relativistic and radiative corrections to the pure Coulomb treatment of both the positronium-ion and di-positronium. Also, work by

Frolov [15], Kinghorn et al. [26], and Suzuki and Usukura [37] have shown that there are actually four stable states of di-positronium - the $L = 0$ ground state, two excited $L = 0$ states, and one $L = 1$ state.

In 1980, Allen P. Mills was able to push forward on the experimental side of things by confirming through observation the existence of the positronium-ion [23]. Mills fired a beam of positrons through a carbon target so that the positrons from the beam could interact with the electrons in the carbon to form positronia atoms and positronium-ions. He was then able to detect the negatively charged positronium-ions by separating them from the neutrally charged positronia atoms and positively charged positrons with a magnetic field. In 2007 Mills and David Cassidy would go on to confirm the existence of di-positronium as well [24]. To do this they fired a beam of positrons into a porous silica film. When the positrons would interact with the electrons in the silica they could form positronia atoms, either in the long-lived triplet state ortho-positronium or the short-lived singlet state para-positronium. Two of these atoms could then interact to form a di-positronium molecule. However, the decay products and decay rate of di-positronium are difficult to distinguish from those of para-positronium so even if di-positronium is created one simply sees a burst of photons from the para-positronium and di-positronium decays followed by a second burst from the ortho-positronium decays. In order to be sure the di-positronium was there at all Mills and Cassidy realized that, unlike the rates of formation of ortho and para-positronia atoms, the formation rate of di-positronium depended on the temperature since it required a third body to transfer momentum to upon creation. This meant that as one increased the temperature it became harder for positronia atoms to interact and form di-positronium. Fewer di-positronium molecules meant more long-lived ortho-positronium atoms. Thus by varying the temperature and finding that the ratio of photons from short-lived state decays (para-positronium and di-positronium) to long-lived state decays (ortho-positronium) increased at lower temperatures they demonstrated that the di-positronium molecule had indeed formed. Nevertheless, experimental studies of the di-positronium are still in the early stages and future investigations could benefit from a stronger base of theoretical knowledge.

## 1.2 Effective Field Theory Methods

As mentioned earlier, an effective field theory can be constructed so as to reproduce the true theory to arbitrarily high precision. The reason that this works is relatively simple. In general, even the best current theory itself is incomplete and only accurately produces physical results up to a certain energy. As one goes to higher energies they probe shorter distances and new phenomena that have not been incorporated in the theory become important. Thus the best current theory is really only capable of making predictions below the energy scale where new physics comes into play. The fact that this theory may give some mathematical description of the short-distance structure is unimportant because the physics that we are interested in, that is the physics at energies accurately described by our theory, cannot probe the short-range details. If we recall the Heisenberg Microscope thought experiment we see that it is essentially the same situation. The processes we are interested in take place up to a particular energy scale meaning they only probe down to a certain length scale. Thus the details of the theory below this length scale cannot be resolved in these processes (see Figure 1). As such, one has the freedom to make certain adjustments

to the theory below this length scale without affecting the physical predictions of the theory.


Figure 1: At a fixed energy a system can only resolve short-range structure down to a certain limit. This lack of resolution can be exploited to replace the complicated true theory (left) with a simple effective model that looks the same at that energy (right).

In the case at hand we are interested in replacing the true theory by a low-energy effective theory. The difference now is that we are observing processes at energies well below the scale where the true theory fails. In other words the physics is not just insensitive to the details beyond the scale where the true theory fails but it is also insensitive to the details of the true theory within a certain regime. We can characterize this regime by introducing a cutoff $\Lambda$ higher than the typical energies of the physical processes involved. This cutoff $\Lambda$ is then used to construct the effective field theory with the idea being that our effective field theory must look identical to the true theory for energies less than $\Lambda$ but for energies greater than $\Lambda$ we can change the theory in any way we like (the logical prescription being to make it easier to work with). However, it is important to remember that the low-energy physics is not entirely insensitive to the short-range structure of our effective theory. We account for this then by including corrections in our effective field theory that mimic the effects of the true short-range behaviour (see Figure 2).

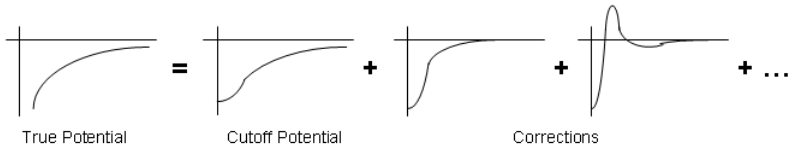


Figure 2: An effective field theory reproduces the true theory by introducing a cutoff potential that simplifies short-range behaviour. A series of corrections can be added to mimic local interactions.

For the case of positronium, as a lowest order approximation, traditional quantum mechanics with a pure Coulomb interaction would be considered the true theory. The Coulomb potential is easy to work with and indeed the dynamics of this problem can be worked out analytically but nevertheless it provides a useful testing ground. In [18] Hill describes the procedure for constructing a low-energy effective field theory for the problem by first introducing a cutoff to eliminate the Coulomb divergence. He then shows that predictions from the effective field theory agree with those from the true theory to arbitrarily high precision by adding in the necessary corrections.

Using an effective field theory does not have any obvious advantage over the true theory when dealing with a Coulomb attraction between two particles because this

problem can be solved analytically. However, when considering scenarios with more complicated interactions or multiple bodies an analytic solution becomes unattainable. Numerical methods become invaluable then to find approximate solutions and this is when using an effective theory can become very useful. By design the effective theory is composed of one or more easy-to-handle pieces which can be processed efficiently numerically.

In this investigation we will further explore the potential benefits of using effective field theories to analyze low-energy systems. The variational methods that we will use to do this are outlined in §2 and following that, in §3, we discuss the numerical techniques we will employ to solve the variational problem effectively. We then move on to test the effective theory against the true theory for the positronium-ion in §4 and for the di-positronium molecule in §5. In both cases we will be primarily interested in comparing the rate of convergence of expectation values for the two methods. The lack of a divergence in our effective field theory means that a Gaussian basis should reproduce the wave function for the effective field theory faster than it does for the true theory. However, the wave function from the effective field theory, despite having converged more than its counterpart for the true theory, will only be useful if we can use it to evaluate expectation values consistent with the true theory faster. For the positronium-ion, in §4, we also take a detour from our discussion of effective field theory methods to calculate a matrix element necessary to determine the order $\alpha^2$ correction to the magnetic moment of the positronium-ion resulting from the interaction between the positron and the two electrons. A thorough discussion of all results is then presented in §6 where we conclude that, for this investigation, using an effective field theory does not speed up the convergence of expectation values. On top of that, the numerical methods used herein can reach beyond the precision for which the effective field theory is designed to be accurate. This means that more corrections need to be calculated for it to be useful and this creates additional work that is not present when using the true theory alone. Ultimately, we cannot show that using effective field theory methods to analyze low-energy systems has any significant advantage over applying the true theory directly but a definitive answer is left to future work.

The software developed for this study works equally well with the effective and with the full theories. It consists of modules encapsulating a Hamiltonian, finding an energy eigenvalue of this Hamiltonian, and optimizing the associated wave function. It is already being used by other students for solving problems with other Hamiltonians, including an exact solution of the three-body problem in one dimension. A thorough discussion of this software can be found in §9.

## 2 Ritz Variational Principle in Non-Orthogonal Basis

In many circumstances one would like to determine the energy spectrum of a quantum system. In almost all such cases it is very difficult or even impossible to analytically solve the Schrödinger equation for these energy levels. However, a simple variational calculation will often yield a set of upper bounds that closely estimate one or more of these energy levels.

### 2.1 Orthonormal Trial Basis

In the simplest scheme one chooses a single normalized trial state $|\psi\rangle$ and computes the expectation of the Hamiltonian with this state. A priori one does not know the eigenstates of the Hamiltonian but there should exist a decomposition of our trial state in this unknown orthonormal basis, call it $|\phi_i\rangle$ (where $\hat{H}|\phi_i\rangle = E_i|\phi_i\rangle$), such that

$$|\psi\rangle = \sum_{i=0}^{\infty} c_i |\phi_i\rangle . \tag{1}$$

Since $|\psi\rangle$ is normalized we have $\sum_{i=0}^{\infty} |c_i|^2 = 1$ and it is straightforward to show that

$$\langle\psi|\hat{H}|\psi\rangle = \sum_{i=0}^{\infty} |c_i|^2 E_i \geq E_0 \sum_{i=0}^{\infty} |c_i|^2 = E_0, \tag{2}$$

thus giving an upper bound on the ground state energy. Often one also makes the trial state dependent on a set of parameters, i.e. $|\psi\rangle = |\psi(\alpha, \beta, ...)\rangle$, so that the upper bound can be extremized at the end of the calculation in terms of these parameters.

Rather than using a single trial state it can be advantageous to use an orthonormal basis of states $\{|\psi_i\rangle, i = 0..(N-1)\}$ where $\langle\psi_i \mid \psi_j\rangle = \delta_{ij}$ . In this case one computes the expectation value of the Hamiltonian for all pairs of basis states. The Schrödinger equation then becomes a matrix equation of the form

$$\langle\psi_i|\hat{H}|\psi_j\rangle\vec{\Phi} = E\vec{\Phi}, \tag{3}$$

which can be treated as a simple eigenvalue problem with $\vec{\Phi}$ being a column vector. Upon solving for the eigenvalues (which we will denote $\left\{\tilde{E}_i, i = 0..(N-1)\right\}$) one can enforce ordering without loss of generality such that

$$\tilde{E}_0 \leq \tilde{E}_1 \leq \tilde{E}_2 \leq ... \tag{4}$$

In this case it becomes clear that $\tilde{E}_0$ would be an upper bound on the ground state energy, $\tilde{E}_1$ an upper bound on the energy of the first excited state, $\tilde{E}_2$ an upper bound on the energy of the second excited state and so on. In this manner if one works in a basis of size $N$ they can get upper bounds on the energies of the first $N$ states.

## 2.2 Non-Orthogonal Trial Basis

Ideally one would like their basis of trial wave functions to look similar to the true wave functions. The closer a trial wave function is to an eigenstate the closer the variational calculation will come to estimating the actual energy of that state. Unfortunately there is not always an obvious choice for an orthogonal basis that accomplishes this. Additionally, depending on the form of the Hamiltonian the matrix elements may be difficult to compute in an orthogonal basis. In this case it is better to work with a simpler set of non-orthogonal trial wave functions.

The variational procedure is only slightly modified when using a non-orthogonal set of trial wave functions. One starts with a set of functions $\left\{\left|\bar{\psi}_i\right\rangle, i = 0..(N-1)\right\}$ and finds matrix elements of the Schrödinger equation.

$$\left\langle\bar{\psi}_i\right| \hat{H} \left|\bar{\psi}_j\right\rangle \vec{\Phi} = E \left\langle\bar{\psi}_i \mid \bar{\psi}_j\right\rangle \vec{\Phi}. \tag{5}$$

The obvious difference now compared to using an orthogonal basis is the presence of an non-trivial overlap matrix (i.e. $\left\langle\bar{\psi}_i \mid \bar{\psi}_j\right\rangle \neq \delta_{ij}$). Consequently we now need to solve a generalized eigenvalue problem (of the form $\overleftrightarrow{A}\vec{v} = \lambda\overleftrightarrow{B}\vec{v}$ where $\overleftrightarrow{A}$ and $\overleftrightarrow{B}$ are both matrices) in order to find the eigenvalues. In theory, this is easily done by simply inverting the overlap matrix and solving the simple eigenvalue problem

$$\left(\left\langle\bar{\psi}_i \mid \bar{\psi}_j\right\rangle\right)^{-1} \left\langle\bar{\psi}_i\right| \hat{H} \left|\bar{\psi}_j\right\rangle \vec{\Phi} = E\vec{\Phi}. \tag{6}$$

In practice, one must also consider the error introduced by performing a certain type of step and matrix inversion can be a very costly process in terms of error. As such, the task of the solving the generalized eigenvalue problem (5) requires some extra thought and various shortcuts exist that simplify this process. We will discuss this problem in more detail in §3.1. The main point is that we are free to perform a variational calculation with a non-orthogonal basis of trial functions and still obtain upper bounds on the energy levels of the system. The only downside is that to do this we would have to solve a generalized eigenvalue problem.

## 2.3 Application to Polyelectrons

The eigenfunctions of the positronium atom with a simple Coulomb potential can be found analytically as with the hydrogen atom. Just like the hydrogen atom they turn out to form a complete orthogonal basis of Hylleraas wave functions. For the positronium-ion and di-positronium molecule one would expect that using a set of Hylleraas wave functions would act as a good orthogonal trial basis for variational calculations. There are two problems with this. First, the fully orthogonalized Hylleraas wave functions become increasingly complicated as we move higher in the basis. This is similar to many orthogonal bases with polynomial coefficients (for example regular polynomials, Hermite polynomials, Laguerre polynomials). If we wish to use Hylleraas functions then we must sacrifice the simplicity that normally comes with using an orthogonal basis. The second problem is that the matrix elements are not easily computed for Hylleraas-type wave functions. For a variational calculation we would like to simplify our calculations as much as possible so Hylleraas wave functions are not well suited to our needs.

Since using an orthogonal basis will only increase the complexity of the calculation of the matrix elements then we are better off switching to a simple non-orthogonal trial basis. We will use Gaussians since the are easy to work with and have the nice property of helping to make integrals easier to solve. The negative aspect of using Gaussians is that they do not have the same limiting behaviours as Hylleraas wave functions which is the type of function we expect would most accurately reflect the true eigenfunctions. That is, Gaussians do not have a cusp at $\vec{r} = 0$ and behave like $e^{-r^2}$ at large distances whereas Hylleraas functions have a cusp and behave like $e^{-r}$ at large distances. Fortunately, for the positronium-ion and the di-positronium molecule, our full basis of Gaussians can be tailored entirely to reproduce the ground state. The hope is that with enough Gaussians we can mimic the short and long-range behaviour closely enough to get a good estimate of the true energy. Meanwhile all of our calculations will have been made much easier by incorporating Gaussians. On the other hand, Gaussian functions will be ideally suited to the effective field theory approach. There is still the issue of long-range behaviour but, nevertheless, we expect that for the effective field theory we should be able to approximate the wave function quite accurately with Gaussians, since the long-range region's contribution is relatively unimportant.

## 3 Numerical Analysis

A single variational calculation with a randomly chosen set of non-orthogonal trial wave functions $\{|\psi_i\rangle\,; i = 0..(N-1)\}$ is unlikely to give a good estimate of the energy of the system. A better approach is to allow the wave functions to depend on a set of parameters $|\psi_i\rangle = |\psi\,(a_i, b_i, c_i, ...)\rangle$. The variational problem then constitutes solving a matrix equation whose parts depend on these parameters.

$$\overleftrightarrow{H}\,|\Phi\rangle = E\,(a_i, b_i, ...; i = 0..(N-1))\,\overleftrightarrow{W}\,|\Phi\rangle\,, \tag{7}$$

where

$$\overleftrightarrow{H} = \overleftrightarrow{H}\,(a_i, b_i, ...; i = 0..(N-1)) = \langle\psi_i|\,\hat{H}\,|\psi_j\rangle$$

and

$$\overleftrightarrow{W} = \overleftrightarrow{W}\,(a_i, b_i, ...; i = 0..(N-1)) = \langle\psi_i\mid\psi_j\rangle\,.$$

Since the eigenvalues of the problem now depend on the parameters, these parameters can be adjusted so as to minimize the eigenvalues and improve the upper bounds on the actual energies of the system.

For the positronium-ion there is only one stable zero angular momentum state. For the di-positronium molecule, there are also two excited $S$-states but we will here be interested only in the ground state. We can thus focus our attention on solving the generalized eigenvalue problem for just one eigenvalue. Furthermore, we know a priori roughly what the energies of these states are. This makes the method of inverse iteration ideal for solving this problem.

### 3.1 Generalized Eigenvalue Problem

#### Inverse Iteration

To solve the generalized eigenvalue problem

$$\overleftrightarrow{H}\,|\Phi\rangle = E\overleftrightarrow{W}\,|\Phi\rangle \tag{8}$$

for a single energy (eigenvalue) $E$ we begin with an estimate of this energy, $E_0$, and a normalized trial eigenvector, $|\psi_0\rangle$. Then consider the linear system

$$\left(\overleftrightarrow{H} - E_0\overleftrightarrow{W}\right)|\chi_0\rangle = \overleftrightarrow{W}\,|\psi_0\rangle\,. \tag{9}$$

The vector $|\chi_0\rangle$ will be closer to the true eigenvector corresponding to the energy $E$ than $|\psi_0\rangle$ was (see [33]). We can see why this is by writing both eigenvectors in the eigenbasis, denoted $|\phi_i\rangle$, with respective eigenvalues $\epsilon_i$,

$$|\psi_0\rangle = \sum_i \alpha_i\,|\phi_i\rangle \qquad |\chi_0\rangle = \sum_i \beta_i\,|\phi_i\rangle\,.$$

If we insert these decompositions into equation (9) we find

$$\beta_i = \frac{\alpha_i}{\epsilon_i - E_0},$$

and

$$|\chi_0\rangle = \sum_i \frac{\alpha_i}{\epsilon_i - E_0} |\phi_i\rangle .$$

Since $(\epsilon_i - E_0)^{-1}$ is very large when $|\phi_i\rangle$ is the eigenvector we are interested in finding then, provided the eigenvalues are well-separated, $|\chi_0\rangle$ will quickly converge to the true eigenvector. Our new and old eigenvectors, $|\chi_0\rangle$ and $|\psi_0\rangle$, can then be used to find an updated estimate on the energy, $E_1$, which will be closer to $E$ than $E_0$ was also. We can then normalize the new vector

$$|\psi_1\rangle \equiv \frac{|\chi_0\rangle}{\sqrt{\langle\chi_0 \mid \chi_0\rangle}}, \tag{10}$$

and solve equation (9) again to obtain a further improved estimate of the eigenenergy and eigenvector. This process can be repeated to determine the eigenenergy with arbitrarily high precision. Also, since each iteration increases the dependence of our trial eigenvector on the true eigenvector by a factor of $(\epsilon_i - E_0)^{-1}$ this process is very fast.

To see how we update the energy consider the $k$-th iteration where we must solve

$$\left(\overleftrightarrow{H} - E_k \overleftrightarrow{W}\right) |\chi_k\rangle = \overleftrightarrow{W} |\psi_k\rangle . \tag{11}$$

For the actual eigenvector $|\Phi\rangle$, equation (8) tells us

$$\left(\overleftrightarrow{H} - E_k \overleftrightarrow{W}\right) |\Phi\rangle = (E - E_k) \overleftrightarrow{W} |\Phi\rangle . \tag{12}$$

The improved eigenvector $|\chi_k\rangle$ should also approximately satisfy this equation so that

$$\overleftrightarrow{W} |\psi_k\rangle \approx (E - E_k) \overleftrightarrow{W} |\chi_k\rangle , \tag{13}$$

where we have used equation (11) on the left side. Taking this equation to be exact gives us a formula for an improved energy rather than the actual energy,

$$\overleftrightarrow{W} |\psi_0\rangle = (E_{k+1} - E_k) \overleftrightarrow{W} |\chi_0\rangle , \tag{14}$$

or

$$E_{k+1} = E_k + \frac{\langle\chi_0| \overleftrightarrow{W} |\psi_0\rangle}{\langle\chi_0| \overleftrightarrow{W} |\chi_0\rangle}. \tag{15}$$

**QR Decomposition**

Inverse iteration now gives us a method to solve the generalized eigenvalue problem very efficiently provided we can solve equation (11) for $|\chi_k\rangle$. There are many ways to do this but we will use QR decomposition for reasons that will be clear later. In QR decomposition the goal is to decompose a matrix into the product of an orthogonal matrix $\overleftrightarrow{Q}$ (i.e. $\overleftrightarrow{Q}\overleftrightarrow{Q}^T = \overleftrightarrow{Q}^T\overleftrightarrow{Q} = \overleftrightarrow{I}$) and an upper triangular matrix $\overleftrightarrow{R}$. In our case, at the $k$-th step, we would like to find the matrices $\overleftrightarrow{Q}_k$ and $\overleftrightarrow{R}_k$ satisfying

$$\overleftrightarrow{Q}_k \overleftrightarrow{R}_k = \overleftrightarrow{H} - E_k \overleftrightarrow{W}. \tag{16}$$

This is a fairly standard procedure and we use the Numerical Recipes routine *NR::qrdcmp* to carry it out. Once we have these two matrices we can apply $\overleftrightarrow{Q}_k^T$ to either side of equation (17) to give

$$\overleftrightarrow{R}_k |\chi_k\rangle = \overleftrightarrow{Q}_k^T \overleftrightarrow{W} |\psi_k\rangle . \tag{17}$$

This equation can now be easily solved via back-substitution for $|\chi_k\rangle$ given that $\overleftrightarrow{R}_k$ is upper triangular. As discussed above, the component of the new eigenvector in the direction of the true eigenvector improves by a factor of $(E - E_0)^{-1}$ at each step so we need only to repeat this process a few times to find an eigenvalue and eigenvector that agree with the actual ones to very high precision.

Repeating this process after updating the energy according to equation (15) will produce the actual eigenenergy and eigenvector correct to whatever precision is required. This eigenvalue then gives us an upper bound on the eigenenergy for our physical system based on the current basis of trial wave functions.

It should be pointed out that one does not need to update the energy after each iteration and often is it best not to. This is because the QR decomposition takes time of the order $N^3$ and each time the energy is updated the full QR decomposition must be recalculated. On the other hand, once a QR decomposition is known, equation (17) can be solved for a new vector quickly. If one repeats this process several times without updating the energy then the resulting vectors will give a more accurate estimate of how to update the energy. In other words, equation (15) becomes more effective with better tuned vectors.

### 3.2 Eigenvalue Minimization

Since the variational method can only determine an upper bound to the true energy, it is crucial that we use a good set of trial wave functions. By introducing a set of parameters into each trial wave function we can search for a set of parameters that minimizes the upper bound on the true energy. As we saw above in equation (7), when we let our trial wave function depend on a set of parameters, $|\psi_i\rangle = |\psi(a_i, b_i, ...)\rangle$, the eigenvalues of the problem become dependent on this set of parameters, $E = E(a_i, b_i, ...; i = 0..(N-1))$. Now what we need is a routine that can effectively adjust these parameters to seek out a minimum value for $E$.

Naively we could define a function that solves the generalized eigenvalue problem (as described in §3.1) and returns the eigenenergy and finally minimizes this function. The problem with this is that changing a parameter in the $k$-th trial wave function will alter the $k$-th row and $k$-th column of $\left(\overleftrightarrow{H} - E\overleftrightarrow{W}\right)$. This would mean each time we evaluate the function we would need to find a new QR decomposition and in turn the new energy at a cost in time of $\mathcal{O}\left(N^3\right)$. If we wish to work with a large basis of trial wave functions then we will have to do better than this.

#### Updating a QR Decomposition

This is where choosing to use QR decomposition to solve the generalized eigenvalue problem comes in very useful. It turns out that if you have already QR decomposed a matrix $\overleftrightarrow{A}$ such that

$$\overleftrightarrow{A} = \overleftrightarrow{Q}\overleftrightarrow{R}$$

and you make a change to $\overleftrightarrow{A}$ of the form

$$\overleftrightarrow{A} \to \overleftrightarrow{A} + \vec{s} \otimes \vec{t}$$

then the QR decomposition can be updated in time of $\mathcal{O}\left(N^2\right)$ [33] (a routine for doing this is provided by Numerical Recipes). As mentioned, when we change a parameter in the $k$-th trial wave function it affects only the $k$-th row and $k$-th column of $\overleftrightarrow{Q}\overleftrightarrow{R} = \left(\overleftrightarrow{H} - E\overleftrightarrow{W}\right)$. Thus the change in the QR decomposition can be written in the form

$$\overleftrightarrow{Q}\overleftrightarrow{R} \to \overleftrightarrow{Q}\overleftrightarrow{R} + \vec{s} \otimes \vec{e}_k + \vec{e}_k \otimes \vec{t}, \tag{18}$$

for two vectors $\vec{s}$ and $\vec{t}$ where $\vec{e}_k$ is a unit vector non-zero in the $k$-th entry only. The QR update scheme can then be applied twice to give the updated QR decomposition

$$\overleftrightarrow{Q}'\overleftrightarrow{R}' = \overleftrightarrow{Q}\overleftrightarrow{R} + \vec{s} \otimes \vec{e}_k + \vec{e}_k \otimes \vec{t}. \tag{19}$$

With the QR decomposition updated for the new parameters we can quickly solve the inverse iteration equation (9) for an updated eigenvector and then use equation (15) to calculate the associated change in energy. A function that calculates the change in energy in this way is what we would now like to minimize.

### Powell's Method

In order to improve the efficiency of the minimization process at each step we will work with all of the parameters for a given wave function rather than dealing with each parameter separately. For example, each trial wave function for the positronium-ion will have three adjustable parameters so, in this case, we will handle each set of three parameters at once. We do this because regardless of how many parameters in a single trial wave function we adjust at a given step, we will only affect one row and one column of the QR decomposition. To deal with this task we will need a minimization scheme that is able to efficiently handle multidimensional problems. Additionally, for a given set of parameters we can only calculate the energy for those exact parameters and have no information about how the energy changes with varying parameters. In others words, we will need a method that does not require gradients of the function being minimized. Powell's method is ideal since it is designed to handle multidimensional problems and avoids the need for derivatives. A thorough discussion of Powell's method can be found in [33] along with source code for executing the routine *NR::powell* which was used in our analysis.

### Growing the Basis

To obtain precise upper bounds on the energies of the positronium-ion and di-positronium systems we will need many trial wave functions in our basis and we will need to fine-tune all wave function parameters. If one begins with a large number of trial functions with random parameters then Powell's method will take a very long time to tune these parameters and find the minimum energy. The trick around this is to grow the basis size during the calculation. In this way we can begin with a small number of trial functions and fine-tune the associated parameters relatively quickly. This gives us a coarsely-tuned set of wave functions with a rough upper

bound on the energy. If we now increase the basis size and include the already coarsely-tuned wave functions then Powell's method can focus on adjusting the new trial functions with only minor adjustments to the old trial functions. This process can be repeated until the desired basis size is reached and a minimum energy is found with high precision. Once the minimization process is finished we can use the tuned parameters and eigenvector to construct the wave function. The wave function can then be used to calculate expectation values for various operators.

# 4 Positronium-ion

We will look first at the three-body positronium-ion system to test the ideas outlined in the previous sections. In particular we will compare the accuracy and rate of convergence of expectation values calculated with an effective field theory versus the true theory. Like any problem in quantum mechanics, writing down the Hamiltonian is a good place to begin. Since the positronium-ion is a relatively low-energy system it suffices to consider a Hamiltonian with only Coulomb interactions to act as the underlying true theory. Thus we can write the Hamiltonian for the positronium-ion as

$$\begin{aligned} \hat{H} &= \left[\frac{\hat{p}_1^2}{2m} + \frac{\hat{p}_2^2}{2m} + \frac{\hat{p}_3^2}{2m}\right] + \left[\frac{\alpha}{r_{12}} - \frac{\alpha}{r_{13}} - \frac{\alpha}{r_{23}}\right] && (20) \\ &= -\frac{1}{2m}\left[\nabla^2_{\vec{A}_1} + \nabla^2_{\vec{A}_2} + \nabla^2_{\vec{A}_3}\right] + \alpha\left[\frac{1}{r_{12}} - \frac{1}{r_{13}} - \frac{1}{r_{23}}\right]. && (21) \end{aligned}$$

We have labeled the particles with the same charge as each other as $\{1,2\}$ and the particle with opposite charge to the first two as $\{3\}$. All particles have the same mass $m$ since they are either electrons or positrons and $\alpha$ denotes the fine structure constant. The kinetic energy operators are naturally defined in terms of the absolute displacements of each particle with respect to the lab frame, denoted $\vec{A}_i$. The potential terms contain the scalar interparticle distances $r_{ij} = \sqrt{\left(\vec{A}_i - \vec{A}_j\right)^2}$. It will be convenient at this point to introduce atomic units. We will from now on measure distances in units $\frac{1}{m\alpha}$, momenta in units $m\alpha$, and energies in units $m\alpha^2$. In these units the Hamiltonian takes the simplified form

$$\hat{H} = -\frac{1}{2}\left[\nabla^2_{\vec{A}_1} + \nabla^2_{\vec{A}_2} + \nabla^2_{\vec{A}_3}\right] + \left[\frac{1}{r_{12}} - \frac{1}{r_{13}} - \frac{1}{r_{23}}\right]. \quad (22)$$

Later on, the trial wave functions that we will use will depend only on the interparticle distances $r_{ij}$. As such it will be necessary to rewrite the kinetic energy operator,

$$\hat{T} = -\frac{1}{2}\left[\nabla^2_{\vec{A}_1} + \nabla^2_{\vec{A}_2} + \nabla^2_{\vec{A}_3}\right], \quad (23)$$

in terms of the interparticle distances rather than absolute coordinates. To accomplish this we introduce the center of mass coordinate

$$\vec{R} = \frac{1}{3}\left(\vec{A}_1 + \vec{A}_2 + \vec{A}_3\right) \quad (24)$$

and two independent relative coordinates

$$\begin{aligned} \vec{r}_{12} &= \vec{A}_2 - \vec{A}_1, && (25) \\ \vec{r}_{13} &= \vec{A}_3 - \vec{A}_1. && (26) \end{aligned}$$

It is straightforward to find the following relations between the gradients of the two coordinate systems

$$\begin{aligned}
\nabla_{\vec{A}_1} &= \frac{1}{3}\nabla_{\vec{R}} - \nabla_{\vec{r}_{12}} - \nabla_{\vec{r}_{13}}, \\
\nabla_{\vec{A}_2} &= \frac{1}{3}\nabla_{\vec{R}} + \nabla_{\vec{r}_{12}}, \\
\nabla_{\vec{A}_3} &= \frac{1}{3}\nabla_{\vec{R}} + \nabla_{\vec{r}_{13}}.
\end{aligned}$$

Thus we can rewrite

$$\begin{aligned}
\hat{T} &= -\frac{1}{2}\left[\nabla^2_{\vec{A}_1} + \nabla^2_{\vec{A}_2} + \nabla^2_{\vec{A}_3}\right] \\
&= -\frac{1}{2}\left[\left(\frac{1}{3}\nabla_{\vec{R}} - \nabla_{\vec{r}_{12}} - \nabla_{\vec{r}_{13}}\right)^2 + \left(\frac{1}{3}\nabla_{\vec{R}} + \nabla_{\vec{r}_{12}}\right)^2 + \left(\frac{1}{3}\nabla_{\vec{R}} + \nabla_{\vec{r}_{13}}\right)^2\right] \\
&= -\frac{1}{2}\left[\frac{1}{3}\nabla^2_{\vec{R}} + 2\nabla^2_{\vec{r}_{12}} + 2\nabla^2_{\vec{r}_{13}} + 2\nabla_{\vec{r}_{12}}\cdot\nabla_{\vec{r}_{13}}\right].
\end{aligned}$$

The term containing $\nabla^2_{\vec{R}}$ corresponds to the kinetic energy of the center-of-mass of the system and has no effect on the internal dynamics of the system so can be omitted. This leaves us with

$$\hat{T} = -\left[\nabla^2_{\vec{r}_{12}} + \nabla^2_{\vec{r}_{13}} + \nabla_{\vec{r}_{12}}\cdot\nabla_{\vec{r}_{13}}\right], \tag{27}$$

giving a Hamiltonian purely in terms of interparticle displacements as

$$\hat{H} = -\left[\nabla^2_{\vec{r}_{12}} + \nabla^2_{\vec{r}_{13}} + \nabla_{\vec{r}_{12}}\cdot\nabla_{\vec{r}_{13}}\right] + \left[\frac{1}{r_{12}} - \frac{1}{r_{13}} - \frac{1}{r_{23}}\right]. \tag{28}$$

### 4.1 Effective Field Theory for the Positronium-ion

The only unattractive feature of the Coulomb potential is the divergence at $\vec{r} = 0$ so we will construct our effective field theory by eliminating this divergence. This is accomplished by introducing a cutoff $\Lambda$ beyond which we will modify the Coulomb potential. The value of the cutoff $\Lambda$ is chosen to be much higher that the typical energies of the system (in momenta units $m\alpha$ this means $\Lambda \gg 1$). The dynamics of the systems are not strongly affected by the physics at energies higher than $\Lambda$ so any way we choose to modify the Coulomb potential in this region will not be devastating to the predictive power of the theory. Let us follow the prescription by Hill in [18] and make the replacement for the potential

$$\frac{1}{r} \to \frac{1}{r}\mathrm{erf}\left(\frac{\Lambda r}{\sqrt{2}}\right) \equiv \hat{V}^{\Lambda}(r). \tag{29}$$

Notice that $\lim_{r\to 0}\hat{V}^{\Lambda}(r) = \sqrt{\frac{2}{\pi}}\Lambda$ so that the modified potential is now finite at $r = 0$ but more importantly this choice preserves the long-range structure of the true theory. It is also useful to observe that in momentum space this is equivalent to multiplying the potential by a Gaussian,

$$\frac{4\pi}{q^2} \to \frac{4\pi}{q^2}\exp\left\{-\frac{q^2}{2\Lambda^2}\right\}. \tag{30}$$

At this point our effective Hamiltonian is

$$\hat{H}^{\Lambda} = \hat{T} + \left[\frac{1}{r_{12}}\mathrm{erf}\left(\frac{\Lambda r_{12}}{\sqrt{2}}\right) - \frac{1}{r_{13}}\mathrm{erf}\left(\frac{\Lambda r_{13}}{\sqrt{2}}\right) - \frac{1}{r_{23}}\mathrm{erf}\left(\frac{\Lambda r_{23}}{\sqrt{2}}\right)\right], \tag{31}$$

but we cannot expect to obtain highly accurate results ignoring the short-range behaviour completely. In order to exactly reproduce the true theory we would need an infinite series of local operators to mimic the short-range interactions which would look something like

$$\begin{aligned}\hat{H}^{\Lambda} = \hat{T} &+ \left[\hat{V}^{\Lambda}(r_{12}) - \hat{V}^{\Lambda}(r_{13}) - \hat{V}^{\Lambda}(r_{23})\right] \\ &+ \frac{d_1}{\alpha^2}\left[\delta^3_{\Lambda}(r_{12}) - \delta^3_{\Lambda}(r_{13}) - \delta^3_{\Lambda}(r_{23})\right] \\ &+ d_2\left[-\nabla^2_{r_{12}}\delta^3_{\Lambda}(r_{12}) + \nabla^2_{r_{13}}\delta^3_{\Lambda}(r_{13}) + \nabla^2_{r_{23}}\delta^3_{\Lambda}(r_{23})\right] \\ &+ d_3\left[\nabla_{r_{12}}\delta^3_{\Lambda}(r_{12})\cdot\nabla_{r_{12}} - \nabla_{r_{13}}\delta^3_{\Lambda}(r_{13})\cdot\nabla_{r_{13}} - \nabla_{r_{23}}\delta^3_{\Lambda}(r_{23})\cdot\nabla_{r_{23}}\right] \\ &+ ...,\end{aligned} \tag{32}$$

where $\delta^3_{\Lambda}$ is a generating function for the local interactions. We are free to choose this function so for simplicity we will use Gaussians such that

$$\delta^3_{\Lambda}(r) = \frac{\alpha^3\Lambda^3}{(2\pi)^{3/2}}\exp\left(\frac{-\Lambda^2 r^2}{2}\right). \tag{33}$$

If we Taylor expand each coefficient $d_i$ in $\alpha$

$$d_i = \alpha d_i^{(1)} + \alpha^2 d_i^{(2)} + \alpha^3 d_i^{(3)} + ... \tag{34}$$

then we can match the effective theory and the true theory in powers of $\alpha$ to determine each $d_i^{(j)}$. One can show that in order to have agreement in energies (in atomic units) between the theories through $\mathcal{O}\left(\alpha^3\right)$ we can set all $d_i^{(j)} = 0$ except for $d_1^{(1)}$ and $d_1^{(2)}$. This degree of precision will be sufficient for our purposes. In [18] Hill uses perturbative matching of scattering amplitudes between the true and effective theories to show that for the Coulomb potential

$$d_1^{(1)} = \frac{2\pi}{\Lambda^2\alpha^2}, \tag{35}$$

$$d_1^{(2)} = \frac{10\sqrt{\pi}}{3\Lambda^3\alpha^3}, \tag{36}$$

when $d_2 = 0$.

For the purpose of finding an approximate wave function for the system we will leave our effective Hamiltonian as

$$\hat{H}^{\Lambda} = \hat{T} + \left[\hat{V}^{\Lambda}(r_{12}) - \hat{V}^{\Lambda}(r_{13}) - \hat{V}^{\Lambda}(r_{23})\right],$$

and later on use the wave function to calculate the lowest order correction

$$\hat{C}^{\Lambda} = \hat{C}^{\Lambda}(r_{12}) - \hat{C}^{\Lambda}(r_{13}) - \hat{C}^{\Lambda}(r_{23}).$$

This should allow us to find energies correct through $\mathcal{O}(\alpha^3)$. To summarize, for the above equations we have

$$\hat{T} = -\left[\nabla^2_{\vec{r}_{12}} + \nabla^2_{\vec{r}_{13}} + \nabla_{\vec{r}_{12}} \cdot \nabla_{\vec{r}_{13}}\right], \tag{37}$$

$$\hat{V}^{\Lambda}(r) = \frac{1}{r}\mathrm{erf}\left(\frac{\Lambda r}{\sqrt{2}}\right), \tag{38}$$

$$C^{\Lambda}(r) \equiv \frac{\Lambda}{\sqrt{2\pi}}\left(1 + \frac{5}{3\sqrt{\pi}\Lambda}\right)\left[\exp\left(-\frac{\Lambda^2 r^2}{2}\right)\right]. \tag{39}$$

### 4.2 Matrix Elements for Positronium-ion

In §2.2 we demonstrated that one could perform a variational calculation using a non-orthogonal basis of trial wave functions, $\{|\psi_i\rangle\}$, to get an upper bound on the energy of the system,

$$\langle\psi_i|\hat{H}|\psi_j\rangle|\Phi\rangle \geq E\langle\psi_i|\psi_j\rangle|\Phi\rangle. \tag{40}$$

As discussed, we will use a basis of Gaussian trial wave functions for our variational calculation that will only depend on the interparticle distances. However, since the system is unchanged under the exchange of the two same-charge particles this must be reflected in our trial wave functions. We will then take the base trial wave function to be

$$\begin{aligned} |\psi_i\rangle &= \exp\left\{-a_i r_{12}^2 - b_i r_{13}^2 - d_i r_{23}^2\right\} + \exp\left\{-a_i r_{12}^2 - d_i r_{13}^2 - b_i r_{23}^2\right\} \\ &\equiv |\psi_i^{12}\rangle + |\psi_i^{21}\rangle. \end{aligned} \tag{41}$$

The parameters $\{a_i, b_i, d_i; i = 0..(N-1)\}$ will be fine-tuned later on during the optimization process in order to improve the upper bound on the eigenenergy. Since we would like to compare results from the effective field theory with those from the true theory we will need to calculate $\langle\psi_i|\psi_j\rangle$, $\langle\psi_i|\hat{H}|\psi_j\rangle$, and $\langle\psi_i|\hat{H}^{\Lambda}|\psi_j\rangle$ and solve the matrix problem in both cases. To simplify this process we will for now consider only the matrix elements $\left\langle\psi_i^{12}|\psi_j^{12}\right\rangle$, $\left\langle\psi_i^{12}\right|\hat{H}\left|\psi_j^{12}\right\rangle$, and $\left\langle\psi_i^{12}\right|\hat{H}^{\Lambda}\left|\psi_j^{12}\right\rangle$ and then later on we can swap parameters in the resulting expressions to obtain all required matrix elements.

Before we begin it will save time later on to obtain an expression for $\hat{T}\left|\psi_i^{12}\right\rangle$. We will use the form of the kinetic energy operator $\hat{T}$ given by equation (37) in terms of gradients with respect to interparticle displacements. Taking gradients of the trial function $\left|\psi_i^{12}\right\rangle$ with respect to $\vec{r}_{12}$ and $\vec{r}_{13}$ we can show

$$\begin{aligned} \nabla_{\vec{r}_{12}}|\psi\rangle &= \left[-2(a+d)\vec{r}_{12} + 2d\vec{r}_{13}\right]|\psi\rangle, \\ \nabla_{\vec{r}_{13}}|\psi\rangle &= \left[2d\vec{r}_{12} - 2(b+d)\vec{r}_{13}\right]|\psi\rangle, \end{aligned}$$

where we have temporarily dropped the wave function and parameter indices. Taking a second gradient gives the various combinations needed to complete the kinetic energy operator,

$$\begin{aligned}
\nabla^2_{\vec{r}_{12}} |\psi\rangle &= \Big[-6\,(a+d) + 4\Big[(a+d)^2\, r_{12}^2 + d^2 r_{13}^2 \\
&\quad -2d\,(a+d)\,\vec{r}_{12}\cdot\vec{r}_{13}]\Big]|\psi\rangle\,, \\
\nabla^2_{\vec{r}_{13}} |\psi\rangle &= \Big[-6\,(b+d) + 4\Big[d^2 r_{12}^2 + (b+d)^2\, r_{13}^2 \\
&\quad -2d\,(b+d)\,\vec{r}_{12}\cdot\vec{r}_{13}]\Big]|\psi\rangle\,, \\
\nabla_{\vec{r}_{12}}\cdot\nabla_{\vec{r}_{13}} |\psi\rangle &= \big[6d + 4\big[-d\,(a+d)\, r_{12}^2 - d\,(b+d)\, r_{13}^2 \\
&\quad + \big(d^2 + (a+d)\,(b+d)\big)\,\vec{r}_{12}\cdot\vec{r}_{13}\big]\big]\,|\psi\rangle\,.
\end{aligned}$$

Adding these up and using the identity $2\vec{r}_{12}\cdot\vec{r}_{13} = r_{12}^2 + r_{13}^2 - r_{23}^2$ (law of cosines) we find

$$\begin{aligned}
\hat{T}\,|\psi\rangle &= \big[6\,(a+b+d) - 2\left(2a^2 + ab + ad - bd\right) r_{12}^2 \\
&\quad -2\left(2b^2 + ab + bd - ad\right) r_{13}^2 \\
&\quad -2\left(2d^2 + ad + bd - ab\right) r_{23}^2\big]\,|\psi\rangle\,. \qquad (42)
\end{aligned}$$

This allows us to break up the matrix element for the kinetic energy operator (restoring indices) as

$$\begin{aligned}
\left\langle\psi_i^{12}\right|\hat{T}\left|\psi_j^{12}\right\rangle &= 6\,(a_i+b_i+d_i)\left\langle\psi_i^{12}|\psi_j^{12}\right\rangle \\
&\quad -2\left(2a_i^2 + a_ib_i + a_id_i - b_id_i\right)\left\langle\psi_i^{12}\right| r_{12}^2\left|\psi_j^{12}\right\rangle \\
&\quad -2\left(2b_i^2 + a_ib_i + b_id_i - a_id_i\right)\left\langle\psi_i^{12}\right| r_{13}^2\left|\psi_j^{12}\right\rangle \\
&\quad -2\left(2d_i^2 + a_id_i + b_id_i - a_ib_i\right)\left\langle\psi_i^{12}\right| r_{23}^2\left|\psi_j^{12}\right\rangle\,. \qquad (43)
\end{aligned}$$

In order to determine the matrix elements for the exact potential we will need to find

$$\left\langle\psi_i^{12}\right|\hat{V}\left|\psi_j^{12}\right\rangle = \left\langle\psi_i^{12}\right|\frac{1}{r_{12}}\left|\psi_j^{12}\right\rangle - \left\langle\psi_i^{12}\right|\frac{1}{r_{13}}\left|\psi_j^{12}\right\rangle - \left\langle\psi_i^{12}\right|\frac{1}{r_{23}}\left|\psi_j^{12}\right\rangle\,. \qquad (44)$$

The cutoff potential is, of course, also easily broken up into three parts

$$\begin{aligned}
\left\langle\psi_i^{12}\right|\hat{V}^{\Lambda}\left|\psi_j^{12}\right\rangle &= \left\langle\psi_i^{12}\right|\frac{1}{r_{12}}\mathrm{erf}\left(\frac{\Lambda r_{12}}{\sqrt{2}}\right)\left|\psi_j^{12}\right\rangle \\
&\quad -\left\langle\psi_i^{12}\right|\frac{1}{r_{13}}\mathrm{erf}\left(\frac{\Lambda r_{13}}{\sqrt{2}}\right)\left|\psi_j^{12}\right\rangle \\
&\quad -\left\langle\psi_i^{12}\right|\frac{1}{r_{23}}\mathrm{erf}\left(\frac{\Lambda r_{23}}{\sqrt{2}}\right)\left|\psi_j^{12}\right\rangle\,. \qquad (45)
\end{aligned}$$

Finally, the correction terms can be divided up

$$\left\langle \psi_i^{12} \right| \hat{C}^{\Lambda} \left| \psi_j^{12} \right\rangle = \frac{\Lambda}{\sqrt{2\pi}} \left( 1 + \frac{5}{3\sqrt{\pi}\Lambda} \right) \left[ \left\langle \psi_i^{12} \right| \exp\left( \frac{-\Lambda^2 r_{12}^2}{2} \right) \left| \psi_j^{12} \right\rangle - \left\langle \psi_i^{12} \right| \exp\left( \frac{-\Lambda^2 r_{13}^2}{2} \right) \left| \psi_j^{12} \right\rangle - \left\langle \psi_i^{12} \right| \exp\left( \frac{-\Lambda^2 r_{23}^2}{2} \right) \left| \psi_j^{12} \right\rangle \right]. \quad (46)$$

As a additional test, we will look at the convergence of expectation values calculated with the wave functions we obtain. In particular, we will consider the electron-positron contact density which is used to determine annihilation rates. Since the first and second particle are identical we need only consider the operator $\delta^3(\vec{r}_{13})$. Thus, we will also need to calculate

$$\left\langle \delta^3(\vec{r}_{13}) \right\rangle = \left\langle \psi_i^{12} \right| \delta^3(\vec{r}_{13}) \left| \psi_j^{12} \right\rangle. \quad (47)$$

It remains now to perform the integrations that will give analytic forms for these matrix elements in terms of the parameters.

### 4.3 Coordinate Shift Approach for Gaussian Integrals

To begin let us consider the overlap integral

$$\langle \chi_i | \chi_j \rangle = \int \mathrm{d}^3\vec{A}_1 \mathrm{d}^3\vec{A}_2 \mathrm{d}^3\vec{A}_3 \, e^{-ar_{12}^2 - br_{13}^2 - dr_{23}^2}, \quad (48)$$

where $a = a_i + a_j$, $b = b_i + b_j$, and $d = d_i + d_j$ when $|\chi_i\rangle = \left|\psi_i^{12}\right\rangle$ and $|\chi_j\rangle = \left|\psi_j^{12}\right\rangle$. The full matrix elements can be obtained from this integral by changing the definitions of $a$, $b$, and $d$. The vectors $\vec{A}_i$ are the absolute coordinates of the particles in the lab frame. The integration measure above is the most general possible and covers all possible positions of the three particles over all space. In fact, we only need to integrate over all possible configurations and we can disregard the position and motion of the center-of-mass in space since this has no physical significance without an external potential.

First let us move to centre-of-mass coordinates $\vec{R}_i$ defined by $\vec{A}_i = \vec{R} + \vec{R}_i$ and $\vec{R} = \frac{1}{3}\left(\vec{A}_1 + \vec{A}_2 + \vec{A}_3\right)$. It is straightforward to compute the Jacobian for this transformation

$$\frac{\partial\left(\vec{A}_1, \vec{A}_2, \vec{A}_3\right)}{\partial\left(\vec{R}_1, \vec{R}_2, \vec{R}\right)} = 3^3. \quad (49)$$

In centre-of-mass coordinates then our volume element becomes

$$3^3 \mathrm{d}^3\vec{R}_1 \mathrm{d}^3\vec{R}_2. \quad (50)$$

We have omitted integration over $\mathrm{d}^3\vec{R}$ since the trial wave function does not depend on the center-of-mass coordinate $\vec{R}$ and the resulting divergent integral will be canceled out upon normalization.

Moving next to relative coordinates defined by $\vec{r}_{12} = \vec{R}_2 - \vec{R}_1$ and $\vec{r}_{13} = \vec{R}_3 - \vec{R}_1$ one can show the Jacobian of this transformation to be

$$\frac{\partial\left(\vec{R}_1, \vec{R}_2\right)}{\partial\left(\vec{r}_{12}, \vec{r}_{13}\right)} = 3^{-3}. \tag{51}$$

We can now rewrite the overlap integral with an integration measure suitable to the integrand as

$$\begin{aligned} \langle \chi_i | \chi_j \rangle &\equiv I(a,b,d) && (52) \\ &= \int \mathrm{d}^3\vec{r}_{12}\mathrm{d}^3\vec{r}_{13}\, e^{-ar_{12}^2 - br_{13}^2 - dr_{23}^2}. && (53) \end{aligned}$$

In order to solve this integral consider the coordinate shift

$$\begin{aligned} \vec{r}_{12} &= \vec{x} + m\vec{y}, \\ \vec{r}_{13} &= \vec{y}, \end{aligned} \tag{54}$$

with unit Jacobian for some constant $m$ yet to be determined. With these coordinates we can rewrite

$$\vec{r}_{23} = \vec{r}_{13} - \vec{r}_{12} = -\vec{x} + (1-m)\,\vec{y}.$$

The argument of the exponential in (53) then becomes

$$\begin{aligned} -ar_{12}^2 - br_{13}^2 - dr_{23}^2 &= -a\left[x^2 + m^2y^2 + 2m\vec{x}\cdot\vec{y}\right] - b\left[y^2\right] \\ &\quad -d\left[x^2 + (1-m)^2\, y^2 - 2\,(1-m)\,\vec{x}\cdot\vec{y}\right]. \end{aligned} \tag{55}$$

We are now free to choose our parameter $m$ so that all dot products in the $(\vec{x}, \vec{y})$ coordinates vanish. In order to make this determination we must solve for arbitrary $\vec{x}, \vec{y}$ the simple equation

$$(\vec{x}\cdot\vec{y})\,[am - d\,(1-m)] = 0, \tag{56}$$

which tells us to choose

$$m = \frac{d}{a+d}. \tag{57}$$

With this choice for $m$, equation (55) can be rewritten

$$\begin{aligned} -ar_{12}^2 - br_{13}^2 - dr_{23}^2 &= -a\left[x^2 + m^2y^2\right] - b\left[y^2\right] - d\left[x^2 + (1-m)^2\, y^2\right] \\ &= -x^2\,[a+d] - y^2\left[\frac{ab + ad + bd}{a+d}\right] \\ &\equiv -\alpha_x x^2 - \alpha_y y^2, \end{aligned} \tag{58}$$

where we have introduced the coefficients

$$\begin{aligned}\alpha_x &= a+d\,,\\ \alpha_y &= \frac{ab+ad+bd}{a+d}.\end{aligned}$$

**Overlap Matrix Elements**

This now allows us to work out the overlap integral quite easily. Rewriting equation (53) as simply

$$I(a,b,d) = \int \mathrm{d}^3\vec{x}\mathrm{d}^3\vec{y}\, e^{-\alpha_x x^2-\alpha_y y^2}, \tag{59}$$

it is trivial to obtain

$$\begin{aligned}I(a,b,d) &= \frac{\pi^3}{(\alpha_x\alpha_y)^{3/2}}\\ &= \frac{\pi^3}{(ab+ad+bd)^{3/2}} \qquad (60)\\ &= \frac{\pi^3}{\left[(a_i+a_j)(b_i+b_j)+(a_i+a_j)(d_i+d_j)+(b_i+b_j)(d_i+d_j)\right]^{3/2}}.\end{aligned}$$

Here we have evaluated only a piece of the overlap matrix element when $|\chi_i\rangle = \left|\psi_i^{12}\right\rangle$ and $|\chi_j\rangle = \left|\psi_j^{12}\right\rangle$. The full overlap matrix element is given by

$$\begin{aligned}\langle\psi_i|\psi_j\rangle &= \langle\psi_i^{12}|\left(1+\hat{P}_{12}\right)^2|\psi_j^{12}\rangle \qquad (61)\\ &= 2\left[\langle\psi_i^{12}|\psi_j^{12}\rangle+\langle\psi_i^{12}|\psi_j^{21}\rangle\right] \qquad (62)\\ &= \frac{2\pi^3}{\left[(a_i+a_j)(b_i+b_j)+(a_i+a_j)(d_i+d_j)+(b_i+b_j)(d_i+d_j)\right]^{3/2}}\\ &\quad+\frac{2\pi^3}{\left[(a_i+a_j)(b_i+d_j)+(a_i+a_j)(d_i+b_j)+(b_i+d_j)(d_i+b_j)\right]^{3/2}},\end{aligned}$$

where $\hat{P}_{12}$ is the permutation operator swapping the first and second particles.

**Exact Coulomb Potential Matrix Elements**

It turns out we can work out all of the other matrix elements that we will need by simple modifications of the above integration. Let us next work out the matrix element for the exact Coulomb potential terms. Given the choice of coordinates (54) we can most easily work out the integral

$$V_{13}(a,b,d) \equiv \int \mathrm{d}^3\vec{r}_{12}\mathrm{d}^3\vec{r}_{13}\left(\frac{1}{r_{13}}\right)e^{-ar_{12}^2-br_{13}^2-dr_{23}^2}, \tag{63}$$

which transforms simply to

$$
\begin{aligned}
V_{13}(\alpha_x, \alpha_y) &= \int \mathrm{d}^3\vec{x}\mathrm{d}^3\vec{y} \left(\frac{1}{y}\right) e^{-\alpha_x x^2 - \alpha_y y^2} && (64)\\
&= \frac{\pi^{3/2}}{(\alpha_x)^{3/2}} \int \mathrm{d}^3\vec{y} \left(\frac{1}{y}\right) e^{-\alpha_y y^2} && (65)\\
&= \frac{4\pi^{5/2}}{(\alpha_x)^{3/2}} \int_0^\infty \mathrm{d}y\, y\, e^{-\alpha_y y^2} && (66)\\
&= \frac{2\pi^{5/2}}{(ab + ad + bd)\sqrt{a+d}}. && (67)
\end{aligned}
$$

Using this result we can quickly find the other exact Coulomb integrals by parameter swapping. For example

$$
\begin{aligned}
V_{12}(\mathbf{a}, \mathbf{b}, d) &= \int \mathrm{d}^3\vec{r}_{12}\mathrm{d}^3\vec{r}_{13} \left(\frac{1}{r_{12}}\right) e^{-\mathbf{a}r_{12}^2 - \mathbf{b}r_{13}^2 - dr_{23}^2} && (68)\\
&= \int \mathrm{d}^3\vec{r}_{13}\mathrm{d}^3\vec{r}_{12} \left(\frac{1}{r_{12}}\right) e^{-\mathbf{b}r_{13}^2 - \mathbf{a}r_{12}^2 - dr_{23}^2} && (69)\\
&= \int \mathrm{d}^3\vec{r}_{12}\mathrm{d}^3\vec{r}_{13} \left(\frac{1}{r_{13}}\right) e^{-\mathbf{b}r_{12}^2 - \mathbf{a}r_{13}^2 - dr_{23}^2} && (70)\\
&\equiv V_{13}(\mathbf{b}, \mathbf{a}, d). && (71)
\end{aligned}
$$

From equation (68) to (69) we simply rearrange the integral so that $\vec{r}_{12}$ takes the role of $\vec{r}_{13}$ in equation (63). Then to get to (70) we simply change the indices (in this case swapping $2 \leftrightarrow 3$) so as to relate this integral to the one we already know. Similarly, one can show

$$
V_{23}(a, \mathbf{b}, \mathbf{d}) = V_{13}(a, \mathbf{d}, \mathbf{b}). \quad (72)
$$

As with the overlap integral we have only been using one part of the wave function so this result only gives us the matrix element

$$
\begin{aligned}
\left\langle \psi_i^{12} \right| \frac{1}{r_{12}} - \frac{1}{r_{13}} - \frac{1}{r_{23}} \left| \psi_j^{12} \right\rangle &= \frac{2\pi^{5/2}}{(ab + ad + bd)} \\
&\quad \times \left[ \frac{1}{\sqrt{b+d}} - \frac{1}{\sqrt{a+b}} - \frac{1}{\sqrt{a+d}} \right], \quad (73)
\end{aligned}
$$

where $a = a_i + a_j$, $b = b_i + b_j$, and $d = d_i + d_j$. The full matrix element for the exact potential is just the sum of four terms like equation (73) with the choices for the parameters for each as

$$
\begin{aligned}
(1) \quad a &= a_i + a_j,\, b = b_i + b_j,\, d = d_i + d_j, && (74)\\
(2) \quad a &= a_i + a_j,\, b = b_i + d_j,\, d = d_i + b_j, && (75)\\
(3) \quad a &= a_i + a_j,\, b = d_i + b_j,\, d = b_i + d_j, && (76)\\
(4) \quad a &= a_i + a_j,\, b = d_i + d_j,\, d = b_i + b_j. && (77)
\end{aligned}
$$

**Effective Potential Matrix Elements**

The cutoff potential matrix elements are given by evaluating integrals of the form

$$V_{13}^{\Lambda}(a,b,d) \equiv \int \mathrm{d}^3\vec{r}_{12}\mathrm{d}^3\vec{r}_{13}\left(\frac{1}{r_{13}}\mathrm{erf}\left\{\frac{\Lambda}{\sqrt{2}}r_{13}\right\}\right)e^{-ar_{12}^2-br_{13}^2-dr_{23}^2},$$

which under the coordinate transformation (54) gives

$$\begin{aligned} V_{13}^{\Lambda}(a,b,d) &= \int \mathrm{d}^3\vec{x}\mathrm{d}^3\vec{y}\left(\frac{1}{y}\mathrm{erf}\left\{\frac{\Lambda}{\sqrt{2}}y\right\}\right)e^{-\alpha_x x^2-\alpha_y y^2} \\ &= \frac{\pi^{3/2}}{(\alpha_x)^{3/2}}\int \mathrm{d}^3\vec{y}\left(\frac{1}{y}\mathrm{erf}\left\{\frac{\Lambda}{\sqrt{2}}y\right\}\right)e^{-\alpha_y y^2} \\ &= \frac{4\pi^{5/2}}{(\alpha_x)^{3/2}}\int_0^{\infty}\mathrm{d}y\, y\,\mathrm{erf}\left\{\frac{\Lambda}{\sqrt{2}}y\right\}e^{-\alpha_y y^2} \\ &= \frac{2\pi^{5/2}}{(ab+ad+bd)\sqrt{(a+d)+\frac{2(ab+ad+bd)}{\Lambda^2}}}. \end{aligned} \tag{78}$$

Using the same tricks as in (68-71) it is straightforward to show

$$V_{12}^{\Lambda}(\mathbf{a},b,\mathbf{d}) = V_{13}^{\Lambda}(\mathbf{b},\mathbf{a},d), \tag{79}$$

$$V_{23}^{\Lambda}(a,\mathbf{b},\mathbf{d}) = V_{13}^{\Lambda}(a,\mathbf{d},\mathbf{b}). \tag{80}$$

We construct the full effective potential matrix element, as we did with equation (73) for the exact potential, by adding up terms of the form (78) for the parameter choices (74-77).

**Effective Potential Correction Matrix Elements**

To find the matrix elements for the correction terms to the effective potential we need to evaluate

$$\begin{aligned} C_{13}^{\Lambda}(a,b,d) &\equiv \int \mathrm{d}^3\vec{r}_{12}\mathrm{d}^3\vec{r}_{13}\left(\exp\left\{-\frac{\Lambda^2}{2}r_{13}^2\right\}\right)e^{-ar_{12}^2-br_{13}^2-dr_{23}^2} \\ &= \int \mathrm{d}^3\vec{r}_{12}\mathrm{d}^3\vec{r}_{13}\, e^{-ar_{12}^2-\left(b+\frac{\Lambda^2}{2}\right)r_{13}^2-dr_{23}^2} \\ &\equiv I\left(a,\left(b+\frac{\Lambda^2}{2}\right),d\right). \end{aligned} \tag{81}$$

This is simply the overlap integral with a shift in the parameter corresponding to the scalar distance involved in the correction. In this manner we can show

$$C_{12}^{\Lambda}(\mathbf{a},b,d) = I\left(\left(\mathbf{a}+\frac{\mathbf{\Lambda^2}}{\mathbf{2}}\right),b,d\right), \tag{82}$$

$$C_{23}^{\Lambda}(a,b,\mathbf{d}) = I\left(a,b,\left(\mathbf{d}+\frac{\mathbf{\Lambda^2}}{\mathbf{2}}\right)\right), \tag{83}$$

and again we construct the full correction matrix element as we did in equation (73) for the exact potential by adding up terms of the form (81) for the parameter choices (74-77).

**Kinetic Energy Matrix Elements**

Based on equation (92) we can see that in order to compute the matrix elements for the kinetic energy terms we will need the overlap integral $I(a,b,d)$ as well as integrals of the form

$$T_{13}(a,b,d) \equiv \int \mathrm{d}^3\vec{r}_{12}\mathrm{d}^3\vec{r}_{13}\left(r_{13}^2\right) e^{-ar_{12}^2-br_{13}^2-dr_{23}^2}, \tag{84}$$

which in the $(\vec{x},\vec{y})$ coordinate system becomes

$$\begin{aligned} T_{13}(a,b,d) &= \int \mathrm{d}^3\vec{x}\mathrm{d}^3\vec{y}\left(y^2\right) e^{-\alpha_x x^2-\alpha_y y^2} && (85)\\ &= \frac{\pi^{3/2}}{(\alpha_x)^{3/2}}\int \mathrm{d}^3\vec{y}\left(y^2\right) e^{-\alpha_y y^2} && (86)\\ &= \frac{4\pi^{5/2}}{(\alpha_x)^{3/2}}\int_0^\infty \mathrm{d}y\, y^4 e^{-\alpha_y y^2} && (87)\\ &= \frac{3\pi^3}{2\alpha_y\left(\alpha_x\alpha_y\right)^{3/2}} && (88)\\ &= \frac{3\pi^3\left(a+d\right)}{2\left(ab+ad+bd\right)^{5/2}}. && (89) \end{aligned}$$

The other integrals for kinetic energy terms can be found by swapping parameters again. In particular

$$\begin{aligned} T_{12}(\mathbf{a},b,\mathbf{d}) &= T_{13}(\mathbf{b},a,\mathbf{d}), && (90)\\ T_{23}(a,\mathbf{b},\mathbf{d}) &= T_{13}(a,\mathbf{d},\mathbf{b}). && (91) \end{aligned}$$

We now have everything we need to compute the matrix element

$$\begin{aligned} \left\langle\psi_i^{12}\right|\hat{T}\left|\psi_j^{12}\right\rangle &= 6\left(a_j+b_j+d_j\right)\left\langle\psi_i^{12}|\psi_j^{12}\right\rangle \\ &\quad -2\left(2a_j^2+a_jb_j+a_jd_j-b_jd_j\right)\left\langle\psi_i^{12}\right| r_{12}^2\left|\psi_j^{12}\right\rangle \\ &\quad -2\left(2b_j^2+a_jb_j+b_jd_j-a_jd_j\right)\left\langle\psi_i^{12}\right| r_{13}^2\left|\psi_j^{12}\right\rangle \\ &\quad -2\left(2d_j^2+a_jd_j+b_jd_j-a_jb_j\right)\left\langle\psi_i^{12}\right| r_{23}^2\left|\psi_j^{12}\right\rangle, \end{aligned} \tag{92}$$

since $\left\langle\psi_i^{12}\right| r_{13}^2\left|\psi_j^{12}\right\rangle = T_{13}(a_i+a_j,b_i+b_j,d_i+d_j)$, $\left\langle\psi_i^{12}\right| r_{12}^2\left|\psi_j^{12}\right\rangle = T_{12}(a_i+a_j,b_i+b_j,d_i+d_j)$, and $\left\langle\psi_i^{12}\right| r_{23}^2\left|\psi_j^{12}\right\rangle = T_{23}(a_i+a_j,b_i+b_j,d_i+d_j)$ and we worked out $\left\langle\psi_i^{12}|\psi_j^{12}\right\rangle$ in equation (61) above. Then to construct the entire kinetic energy wave function we add together four such pieces with parameters chosen according to equations (74-77).

**Delta Function Matrix Elements**

Finally, the matrix element for the electron-positron contact density is just

$$\begin{aligned}\left\langle \psi_i^{12}\right| \delta^3\left(\vec{r}_{13}\right) \left|\psi_j^{12}\right\rangle &= \int \mathrm{d}^3\vec{r}_{12}\mathrm{d}^3\vec{r}_{13}\delta\left(\vec{r}_{13}\right) e^{-ar_{12}^2-br_{13}^2-dr_{23}^2} &(93)\\ &= \int \mathrm{d}^3\vec{r}_{12} e^{-(a+d)x^2} &(94)\\ &= \frac{\pi^{3/2}}{(a+d)^{3/2}}. &(95)\end{aligned}$$

For the full matrix element we must add up four pieces like this where $a = a_i + a_j$ always but $d$ takes on the definitions

$$\begin{aligned}(1)\quad d &= d_i + d_j,\\ (2)\quad d &= d_i + b_j,\\ (3)\quad d &= b_i + d_j,\\ (4)\quad d &= b_i + b_j.\end{aligned}$$

## 4.4 Magnetic Moment

With the above framework in place it is worthwhile to take a detour from the central theme of this thesis to calculate a matrix element, previously unknown for the positronium-ion, that is necessary to quantify the effect that the interaction between the constituents of the positronium-ion has on its magnetic moment. Naively, we would take the magnetic moment of the positronium-ion to be just that of the positron since the electrons form a spin singlet with no net magnetic moment. The magnetic moment of the system would then be just that of a free positron, that is, $g\frac{\hbar}{2}\frac{e}{2m}$ where $g = 2 + \frac{\alpha}{\pi} + \ldots$ is the gyromagnetic ratio known for the free-particle up to $\mathcal{O}\left(\left(\frac{\alpha}{\pi}\right)^4\right)$ and five-loop effects are being calculated at present [3]. However, for the positronium-ion we expect the interaction between the positron and the electrons to modify this magnetic moment. This effect is similar to that in hydrogen-like atoms and ions where the nuclear electric field modifies the $g$-factor of an electron [6]. We can use this analogy to deduce that such an effect should be a correction of $\mathcal{O}\left(\alpha^2\right)$ enhanced relative to the free-particle effects at this order in the coupling constant by a factor of order $\pi^2$. A more detailed calculation, wherein one expands the Dirac equation describing the dynamics of a charged particle bound with two antiparticles to $\mathcal{O}\left(\alpha^2\right)$, shows that the magnetic interaction in a hydrogen-like atom is described not by the lowest order expression

$$\frac{e}{2m}\sigma\cdot\mathrm{B}, \tag{96}$$

which gives $g = 2$, but rather by [1, 25],

$$\frac{e}{2m}\left(1 - \frac{p^2}{4m^2} - \frac{e}{6m}\varepsilon\cdot\mathrm{r}\right)\sigma\cdot\mathrm{B}. \tag{97}$$

Here, $\varepsilon$ denotes the electric field due to the companion particles. The bound-particle $g$-factor in a hydrogen-like atom then becomes

$$g = 2 \rightarrow g = 2\left(1 - \frac{\langle p^2 \rangle}{2m^2} - \frac{e}{6m}\langle \varepsilon \cdot \mathrm{r} \rangle\right). \tag{98}$$

For a three-body positronium-ion, this formula will have to be modified , but it is likely to also include the expectation value $\langle \varepsilon \cdot \mathrm{r} \rangle$ which, in the case of the positronium-ion, is the expectation value of the scalar product of the electric field that the positron feels times its position vector, as measured from the ion's center of mass. This expectation value, $\langle \varepsilon \cdot \mathrm{r} \rangle$, has yet to be calculated for the positronium-ion so our purpose here will be to do just that.

### Magnetic Moment Matrix Elements

In terms of the notation from previous sections the matrix element of interest can be written $\left\langle \vec{\varepsilon}_3 \cdot \vec{R}_3 \right\rangle$ where $\vec{\varepsilon}_3$ is the electric field as felt by the positron (particle 3) due to the Coulomb fields of the electrons (particles 1 and 2) and $\vec{R}_3$ is the center-of-mass position of the positron. Let us focus on just the electric field from the electron at position 1 for now. This electric field is

$$\vec{\varepsilon}_{13} = -e\frac{\vec{r}_{13}}{r_{13}^3}. \tag{99}$$

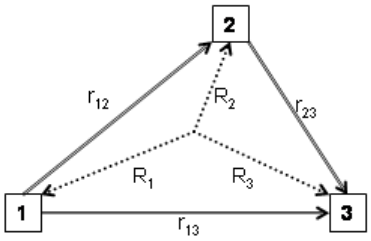


Figure 3: Positronium-ion in center-of-mass coordinates $\vec{R}_i$ and relative coordinates $\vec{r}_{ij} = \vec{R}_j - \vec{R}_i$.

Thus, we will need an expression for $\vec{r}_{13} \cdot \vec{R}_3$. Since the centre of mass of a triangle (see Figure 3) is the intersection of its medians we can deduce the relation $\vec{R}_3 = \frac{1}{3}(\vec{r}_{13} + \vec{r}_{23})$. Therefore

$$\begin{aligned} \vec{r}_{13} \cdot \vec{R}_3 &= \frac{1}{3}\vec{r}_{13} \cdot (\vec{r}_{13} + \vec{r}_{23}) \\ &= \frac{1}{3}\left(r_{13}^2 + \vec{r}_{13} \cdot \vec{r}_{23}\right) \\ &= \frac{1}{2}r_{13}^2 + \frac{1}{6}\left(r_{23}^2 - r_{12}^2\right). \end{aligned}$$

This gives us

$$\left\langle \vec{\varepsilon}_{13} \cdot \vec{R}_3 \right\rangle = -e\left[\frac{1}{2}\left\langle \frac{1}{r_{13}} \right\rangle + \frac{1}{6}\left\langle \frac{r_{23}^2 - r_{12}^2}{r_{13}^3} \right\rangle\right].$$

The field from the electron at position 2 will contribute the exact same amount when averaged with the wave function so we can simply double this result to obtain

$$\left\langle \vec{\varepsilon}_3 \cdot \vec{R}_3 \right\rangle = -e \left[ \left\langle \frac{1}{r_{13}} \right\rangle + \frac{1}{3} \left\langle \frac{r_{23}^2 - r_{12}^2}{r_{13}^3} \right\rangle \right]. \tag{100}$$

We already have an expression for the expectation value of the Coulomb operator in equation (67) above. All that remains then is to calculate the second expectation value. This requires evaluating the integral

$$\left\langle \frac{r_{23}^2 - r_{12}^2}{r_{13}^3} \right\rangle = \int \mathrm{d}^3\vec{r}_{12} \mathrm{d}^3\vec{r}_{13} \left( \frac{r_{23}^2 - r_{12}^2}{r_{13}^3} \right) e^{-ar_{12}^2 - br_{13}^2 - dr_{23}^2}. \tag{101}$$

Notice we can take antiderivatives with respect to parameters $a$ and $d$ to rewrite this as

$$\left\langle \frac{r_{23}^2 - r_{12}^2}{r_{13}^3} \right\rangle = \left( \frac{\mathrm{d}}{\mathrm{d}a} - \frac{\mathrm{d}}{\mathrm{d}d} \right) \int \mathrm{d}^3\vec{r}_{12} \mathrm{d}^3\vec{r}_{13} \left( \frac{1}{r_{13}^3} \right) e^{-ar_{12}^2 - br_{13}^2 - dr_{23}^2}. \tag{102}$$

Making the coordinate change (54) gives

$$\left\langle \frac{r_{23}^2 - r_{12}^2}{r_{13}^3} \right\rangle = \left( \frac{\mathrm{d}}{\mathrm{d}a} - \frac{\mathrm{d}}{\mathrm{d}d} \right) \int \mathrm{d}^3\vec{x} \mathrm{d}^3\vec{y} \left( \frac{1}{y^3} \right) e^{-\alpha_x x^2 - \alpha_y y^2} \tag{103}$$

$$= \left( \frac{\mathrm{d}}{\mathrm{d}a} - \frac{\mathrm{d}}{\mathrm{d}d} \right) \left( \frac{\pi^{3/2}}{\alpha_x^{3/2}} \right) \int \mathrm{d}^3\vec{y} \left( \frac{1}{y^3} \right) e^{-\alpha_y y^2}. \tag{104}$$

It is straightforward to show that

$$\left( \frac{\mathrm{d}}{\mathrm{d}a} - \frac{\mathrm{d}}{\mathrm{d}d} \right) \left( \frac{\pi^{3/2}}{\alpha_x^{3/2}} \right) = 0.$$

We can thus bring the derivative operators inside the integrand so that

$$\left\langle \frac{r_{23}^2 - r_{12}^2}{r_{13}^3} \right\rangle = \frac{\pi^{3/2}}{\alpha_x^{3/2}} \int \mathrm{d}^3\vec{y} \left( \frac{1}{y^3} \right) e^{-\alpha_y y^2} \left( y^2 \left( \frac{\mathrm{d}}{\mathrm{d}d} - \frac{\mathrm{d}}{\mathrm{d}a} \right) \alpha_y \right) \tag{105}$$

$$= \frac{\pi^{3/2}}{\alpha_x^{3/2}} \left( \left( \frac{\mathrm{d}}{\mathrm{d}d} - \frac{\mathrm{d}}{\mathrm{d}a} \right) \alpha_y \right) \int \mathrm{d}^3\vec{y} \left( \frac{1}{y} \right) e^{-\alpha_y y^2} \tag{106}$$

$$= \frac{\pi^{3/2}}{\alpha_x^{3/2}} \left( \frac{a^2 - d^2}{(a+d)^2} \right) \left( \frac{2\pi}{\alpha_y} \right). \tag{107}$$

From line (106) to (107) we have used the relations $\frac{\mathrm{d}\alpha_y}{\mathrm{d}d} = \frac{a^2}{(a+d)^2}$ and $\frac{\mathrm{d}\alpha_y}{\mathrm{d}a} = \frac{d^2}{(a+d)^2}$. Simplifying then gives the desired expectation value

$$\left\langle \frac{r_{23}^2 - r_{12}^2}{r_{13}^3} \right\rangle = \frac{2\pi^{5/2}(a-d)}{(ab + ad + bd)(a+d)^{3/2}}.$$

We are now in a position to calculate $\langle \varepsilon \cdot \mathrm{r} \rangle$ in equation (98) for the positronium-ion.

### 4.5 Results

We can now use the above expressions for the Hamiltonian matrix elements to optimize a parameter set $\{a_i, b_i, d_i; i = 0..(N-1)\}$ using the program described in §3 so as to compare the true and effective theories. First let us look at the convergence of the bound state energy. For the effective field theory we took $\Lambda = 50$. Results for various size bases of trial wave functions are given in Table 1.

| Basis Size ($N$) | EFT at $\mathcal{O}(\alpha)$, $\left\langle \hat{H}^{\Lambda} \right\rangle$ | Correction, $\left\langle \hat{C}^{\Lambda} \right\rangle$ | EFT at $\mathcal{O}(\alpha^3)$, $\left\langle \hat{H}^{\Lambda} \right\rangle + \left\langle \hat{C}^{\Lambda} \right\rangle$ | Exact Theory $\left\langle \hat{H} \right\rangle$ |
|---|---|---|---|---|
| 10 | -0.260710305 | -0.000854119 | -0.260795717 | -0.261471242 |
| 20 | -0.261839109 | -0.000096780 | -0.261935890 | -0.261946028 |
| 40 | -0.261889258 | -0.000099431 | -0.261988689 | -0.261999937 |
| 60 | -0.261903359 | -0.000100691 | -0.262004050 | -0.262003853 |
| 80 | -0.261904266 | -0.000100855 | -0.262005122 | -0.262004316 |
| 100 | -0.261904369 | -0.000100837 | -0.262005206 | -0.262004851 |
| 120 | -0.261904401 | -0.000100836 | -0.262005237 | -0.262004975 |
| 160 | -0.261904437 | -0.000100841 | -0.262005278 | -0.262005036 |
| 200 | -0.261904447 | -0.000100853 | -0.262005301 | -0.262005055 |
| 240 | -0.261904458 | -0.000100846 | -0.262005304 | -0.262005057 |

Table 1: Energy of the positronium-ion bound state in units $m\alpha^2$.

The actual energy of the positronium-ion, given to nine significant digits, was found by Frolov to be $-0.262005070\, m\alpha^2$ [13]. As we can see in the last column of Table 1 all of the energies produced using the true theory are consistent with Frolov's results in the sense that they do not drop below his value. Additionally, as the number of wave functions in the basis increases, the upper bounds converge nicely to his value with agreement to a few parts in $10^8$ for $N = 240$. For the effective field theory we can see that both the uncorrected energy (Table 1: Column 2) and expectation value for the $\mathcal{O}(\alpha^2)$ plus $\mathcal{O}(\alpha^3)$ correction (Table 1: Column 3) converge nicely to a constant value. Consequently, the corrected energy also converges to a constant value (Table 1: Column 4). Unfortunately, this constant value overshoots the actual energy for $N \geq 80$. This is because at this basis size the program can resolve energies to parts per $10^7$ which is where the $\mathcal{O}(\alpha^4)$ correction becomes important. Note, as a consistency check one can show that the next order correction will be positive in agreement with the fact that our results for the effective field theory at $\mathcal{O}(\alpha^3)$ are lower than the actual energy [18].

Comparing the speed of convergence for the two theories (Table 1: Column 3 and 4) we see that the effective field theory actually converges to its final value slightly faster than the true theory. For example, the difference between the $N = 80$ and $N = 240$ for the effective field theory is less than $2 \times 10^{-7}$ meanwhile for the true theory it is slightly more than $7 \times 10^{-7}$ . This is what we would expect since the trial basis is composed of Gaussian wave functions which are better suited to the effective field theory. The more important question, however, is; will the wave function associated with the effective field theory produce expectation values that converge more quickly than the wave function for the true theory? To answer this let us look now at the expectation values for the delta function.

Once the optimization process is finished at a particular basis size we can use the tuned parameters and eigenvector corresponding to the eigenvalues in Table 1 to approximate the wave function for the system. This wave function is then used to calculate the expectation value of the electron-positron contact density (the delta function). Values of this expectation value for various basis sizes are given in Table 2.

| Basis Size ($N$) | $\langle\delta_{e^+e^-}\rangle$ using EFT | $\langle\delta_{e^+e^-}\rangle$ using Exact Theory |
|---|---|---|
| 10 | 0.016835 | 0.017846 |
| 20 | 0.019080 | 0.019250 |
| 40 | 0.019645 | 0.020188 |
| 60 | 0.019963 | 0.020354 |
| 80 | 0.020020 | 0.020438 |
| 100 | 0.020022 | 0.020577 |
| 120 | 0.020029 | 0.020592 |
| 160 | 0.020025 | 0.020663 |
| 200 | 0.020044 | 0.020670 |
| 240 | 0.020029 | 0.020671 |

Table 2: Expectation values of delta function, $\delta_{e^+e^-}$, for positronium-ion.

The actual value for the electron-positron contact density in positronium-ion given to six decimal places is 0.020733 [13]. In both approaches the values are relatively well behaved but the exact theory clearly gives more accurate results. Despite the fact that the values from the effective field theory appear to converge more quickly than those from the true theory, they do not converge to the correct value. Based on the values in Table 2: Column 2 we might estimate that the expectation value of this delta function was roughly $0.02003 \pm \left(2 \times 10^{-5}\right)$. This would be a gross error. The underlying reason for this disagreement is most likely due to the fact that the effective field theory gives rise to a wave function that is smooth at $\vec{r} = 0$. Such a function is not well-suited to probing the divergence of the delta function. On the other hand, the wave function for the true theory takes longer to converge but, in doing so, would attempt to mimic the cusp of the true wave function at $\vec{r} = 0$. This is why the values produced using the true theory (Table 2: Column 3) come much closer to the actual result.

We turn our attention now to the expectation values of the operators needed to calculate the correction to the magnetic moment. We use the wave function produced by the true theory to find the values in Table 3.

For both operators the expectation values converge to constant values. The values from Table 3: Column 2 imply that $\left\langle \frac{1}{r_{13}} \right\rangle = 0.339821 \pm \left(1 \times 10^{-6}\right)\, m\alpha$. This expectation value has actually been worked out to higher precision by Frolov and he reports a value of $0.339821023\, m\alpha$ to nine significant digits [12]. This acts as a good consistency check for our result since they are in agreement. The second operator, on the other hand, has not been worked out to our knowledge and based on our results (Table 3: Column 3) we can estimate that $\left\langle \frac{r_{23}^2 - r_{12}^2}{r_{13}^3} \right\rangle = -0.24687 \pm \left(2 \times 10^{-5}\right)\, m\alpha$. Thus, using Frolov's result for $\left\langle \frac{1}{r_{13}} \right\rangle$ and our value for $\left\langle \frac{r_{23}^2 - r_{12}^2}{r_{13}^3} \right\rangle$ we can infer based

| Basis Size ($N$) | $\left\langle \frac{1}{r_{13}} \right\rangle$ | $\left\langle \frac{r_{23}^2 - r_{12}^2}{r_{13}^3} \right\rangle$ |
|---|---|---|
| 40 | 0.33981484 | -0.2468256 |
| 80 | 0.33982184 | -0.2468704 |
| 120 | 0.33982152 | -0.2468650 |
| 160 | 0.33982116 | -0.2468714 |
| 200 | 0.33982114 | -0.2468671 |
| 240 | 0.33982113 | -0.2468631 |

Table 3: Expectation values needed for calculating the correction to magnetic moment of the positronium-ion in units $m\alpha$.

on equation (100) that

$$\left\langle \vec{\varepsilon}_3 \cdot \vec{R}_3 \right\rangle = -0.25753 \pm \left(1 \times 10^{-5}\right) m\alpha^{3/2}. \tag{108}$$

## 5 Di-positronium Molecule

Let us now move on to the four-body di-positronium molecule to further test the ideas outlined in the previous sections. Once again we will compare the accuracy and speed of convergence of expectation values calculated with the effective field theory and the true theory. Since the di-positronium molecule is a relatively low-energy system it suffices to consider a Hamiltonian with only Coulomb interactions to act as the underlying true theory. Thus we can write the Hamiltonian for the di-positronium molecule as

$$\begin{aligned}\hat{H} &= \left[\frac{\hat{p}_1^2}{2m}+\frac{\hat{p}_2^2}{2m}+\frac{\hat{p}_3^2}{2m}+\frac{\hat{p}_4^2}{2m}\right]+\left[\frac{\alpha}{r_{12}}+\frac{\alpha}{r_{34}}-\frac{\alpha}{r_{13}}-\frac{\alpha}{r_{14}}-\frac{\alpha}{r_{23}}-\frac{\alpha}{r_{24}}\right] \\ &= -\frac{1}{2m}\left[\nabla^2_{\vec{A}_1}+\nabla^2_{\vec{A}_2}+\nabla^2_{\vec{A}_3}+\nabla^2_{\vec{A}_4}\right] \\ &\quad +\alpha\left[\frac{1}{r_{12}}+\frac{1}{r_{34}}-\frac{1}{r_{13}}-\frac{1}{r_{14}}-\frac{1}{r_{23}}-\frac{1}{r_{24}}\right].\end{aligned}$$

We have taken particles $\{1,2\}$ to have the same charge as each other but opposite to that of particles $\{3,4\}$. All particles have the same mass $m$ since they are either electrons or positrons and $\alpha$ denotes the fine structure constant. The kinetic energy operators are naturally defined in terms of the absolute displacements of each particle with respect to the lab frame, denoted $\vec{A}_i$. The potential terms contain the scalar interparticle distances $r_{ij}=\sqrt{\left(\vec{A}_i-\vec{A}_j\right)^2}$. Let us now introduce atomic units such that distances are measured in units $\frac{1}{m\alpha}$, momenta in units $m\alpha$, and energies in units $m\alpha^2$. This change allows us to rewrite the Hamiltonian more simply as

$$\hat{H} = -\frac{1}{2}\left[\nabla^2_{\vec{A}_1}+\nabla^2_{\vec{A}_2}+\nabla^2_{\vec{A}_3}+\nabla^2_{\vec{A}_4}\right]+\left[\frac{1}{r_{12}}+\frac{1}{r_{34}}-\frac{1}{r_{13}}-\frac{1}{r_{14}}-\frac{1}{r_{23}}-\frac{1}{r_{24}}\right]$$

The trial wave functions that we will use later on will depend only on the interparticle distances $r_{ij}$ so it will be useful to rewrite the kinetic energy operator,

$$\hat{T}=-\frac{1}{2}\left[\nabla^2_{\vec{A}_1}+\nabla^2_{\vec{A}_2}+\nabla^2_{\vec{A}_3}+\nabla^2_{\vec{A}_4}\right], \tag{109}$$

in terms of the interparticle distances rather than absolute coordinates. To accomplish this we introduce the center of mass coordinate

$$\vec{R}=\frac{1}{4}\left(\vec{A}_1+\vec{A}_2+\vec{A}_3+\vec{A}_4\right), \tag{110}$$

and three independent relative coordinates

$$\vec{r}_{12} = \vec{A}_2-\vec{A}_1, \tag{111}$$
$$\vec{r}_{13} = \vec{A}_3-\vec{A}_1, \tag{112}$$
$$\vec{r}_{14} = \vec{A}_4-\vec{A}_1. \tag{113}$$

It is straightforward to find the following relations between the gradients in the two

coordinate systems

$$\begin{aligned}
\nabla_{\vec{A}_1} &= \frac{1}{4}\nabla_{\vec{R}} - \nabla_{\vec{r}_{12}} - \nabla_{\vec{r}_{13}} - \nabla_{\vec{r}_{14}}, \\
\nabla_{\vec{A}_2} &= \frac{1}{4}\nabla_{\vec{R}} + \nabla_{\vec{r}_{12}}, \\
\nabla_{\vec{A}_3} &= \frac{1}{4}\nabla_{\vec{R}} + \nabla_{\vec{r}_{13}}, \\
\nabla_{\vec{A}_4} &= \frac{1}{4}\nabla_{\vec{R}} + \nabla_{\vec{r}_{14}}.
\end{aligned}$$

Substituting these into the expression for the kinetic energy operator (109) gives us

$$\begin{aligned}
\hat{T} &= -\frac{1}{2}\left[\nabla^2_{\vec{A}_1} + \nabla^2_{\vec{A}_2} + \nabla^2_{\vec{A}_3} + \nabla^2_{\vec{A}_4}\right] \\
&= -\frac{1}{2}\left[\left(\frac{1}{4}\nabla_{\vec{R}} - \nabla_{\vec{r}_{12}} - \nabla_{\vec{r}_{13}} - \nabla_{\vec{r}_{14}}\right)^2 + \left(\frac{1}{4}\nabla_{\vec{R}} + \nabla_{\vec{r}_{12}}\right)^2\right. \\
&\qquad \left. + \left(\frac{1}{4}\nabla_{\vec{R}} + \nabla_{\vec{r}_{13}}\right)^2 + \left(\frac{1}{4}\nabla_{\vec{R}} + \nabla_{\vec{r}_{14}}\right)^2\right] \\
&= -\frac{1}{2}\left[\frac{1}{4}\nabla^2_{\vec{R}} + 2\nabla^2_{\vec{r}_{12}} + 2\nabla^2_{\vec{r}_{13}} + 2\nabla^2_{\vec{r}_{14}}\right. \\
&\qquad \left. + 2\nabla_{\vec{r}_{12}}\cdot\nabla_{\vec{r}_{13}} + 2\nabla_{\vec{r}_{12}}\cdot\nabla_{\vec{r}_{14}} + 2\nabla_{\vec{r}_{13}}\cdot\nabla_{\vec{r}_{14}}\right].
\end{aligned}$$

We can omit the term containing $\nabla^2_{\vec{R}}$ because it corresponds to the kinetic energy of the center-of-mass of the system and has no effect on the internal dynamics of the system. This leaves us with

$$\hat{T} = -\left[\nabla^2_{\vec{r}_{12}} + \nabla^2_{\vec{r}_{13}} + \nabla^2_{\vec{r}_{14}} + \nabla_{\vec{r}_{12}}\cdot\nabla_{\vec{r}_{13}} + \nabla_{\vec{r}_{12}}\cdot\nabla_{\vec{r}_{14}} + \nabla_{\vec{r}_{13}}\cdot\nabla_{\vec{r}_{14}}\right]$$

We now have a dimensionless Hamiltonian purely in terms of interparticle displacements

$$\begin{aligned}
\hat{H} &= -\left[\nabla^2_{\vec{r}_{12}} + \nabla^2_{\vec{r}_{13}} + \nabla^2_{\vec{r}_{14}} + \nabla_{\vec{r}_{12}}\cdot\nabla_{\vec{r}_{13}} + \nabla_{\vec{r}_{12}}\cdot\nabla_{\vec{r}_{14}} + \nabla_{\vec{r}_{13}}\cdot\nabla_{\vec{r}_{14}}\right] \\
&\quad + \left[\frac{1}{r_{12}} + \frac{1}{r_{34}} - \frac{1}{r_{13}} - \frac{1}{r_{14}} - \frac{1}{r_{23}} - \frac{1}{r_{24}}\right]
\end{aligned}$$

### 5.1 Effective Field Theory the Di-positronium

As with the positronium-ion, we would like to build an effective field theory which does not have the $\vec{r} = 0$ divergence in the Coulomb potential. To accomplish this we will follow the same prescription that we did in §4.1. In particular, we will again use the effective potential in equation (29) in place of the Coulomb potential and we also keep the same generating function, equation (33), to reproduce the short-range behaviour. This means we do not need to recalculate the coefficients, equations (35-36), which make the effective theory correct through $\mathcal{O}\left(\alpha^3\right)$.

Thus, in order to find an approximate wave function for the system in the effective theory case we will take the effective Hamiltonian as

$$\begin{aligned}\hat{H}^{\Lambda} &= \hat{T} + \Big[\hat{V}^{\Lambda}(r_{12}) + \hat{V}^{\Lambda}(r_{34}) - \hat{V}^{\Lambda}(r_{13}) - \hat{V}^{\Lambda}(r_{14}) \\ &\quad -\hat{V}^{\Lambda}(r_{23}) - \hat{V}^{\Lambda}(r_{24})\Big],\end{aligned}$$

and once we have found the wave function for $\hat{H}^{\Lambda}$ we will use it to calculate the correction to the energy,

$$\begin{aligned}\hat{C}^{\Lambda} &= \hat{C}^{\Lambda}(r_{12}) + \hat{C}^{\Lambda}(r_{34}) - \hat{C}^{\Lambda}(r_{13}) \\ &\quad -\hat{C}^{\Lambda}(r_{14}) - \hat{C}^{\Lambda}(r_{23}) - \hat{C}^{\Lambda}(r_{24}).\end{aligned}$$

Recall, in the above equations we have

$$\hat{T} = -\left[\nabla^2_{\vec{r}_{12}} + \nabla^2_{\vec{r}_{13}} + \nabla^2_{\vec{r}_{14}} + \nabla_{\vec{r}_{12}} \cdot \nabla_{\vec{r}_{13}} + \nabla_{\vec{r}_{12}} \cdot \nabla_{\vec{r}_{14}} + \nabla_{\vec{r}_{13}} \cdot \nabla_{\vec{r}_{14}}\right], \tag{114}$$

$$\hat{V}^{\Lambda}(r) = \frac{1}{r}\mathrm{erf}\left(\frac{\Lambda r}{\sqrt{2}}\right), \tag{115}$$

$$C^{\Lambda}(r) \equiv \frac{\Lambda}{\sqrt{2\pi}}\left(1 + \frac{5}{3\sqrt{\pi}\Lambda}\right)\left[\exp\left(-\frac{\Lambda^2 r^2}{2}\right)\right]. \tag{116}$$

### 5.2 Matrix Elements for Di-positronium Molecule

We now need to compute the matrix elements for the di-positronium molecule system with the effective and true theory Hamiltonians using a basis of trial wave functions, $\{|\psi_i\rangle\}$. The variational procedure discussed in §2.2 will then enable us to get an upper bound on the energy of the system since

$$\langle\psi_i|\,\hat{H}\,|\psi_j\rangle\,|\Phi\rangle \geq E\,\langle\psi_i|\psi_j\rangle\,|\Phi\rangle\,. \tag{117}$$

As discussed, we will use a basis of Gaussian trial wave functions for our variational calculation that will only depend on the interparticle distances. In constructing the trial wave function we must take into account the symmetries of the system. In particular, our trial wave function must reflect: (1) that the dynamics are unchanged by swapping two same-charge particles and (2) we are free to invert the charges of all the particles simultaneously without affecting the system's dynamics. Let us denote the electrons as particles $\{1,2\}$ and the positrons as particles $\{3,4\}$. To see how we will construct the full trial wave function let us start out with what will end up just being a piece of the final result. Consider

$$\begin{aligned}\left|\psi_i^{1234}\right\rangle &\equiv \phi(a_i, b_i, c_i, d_i, e_i, f_i) \\ &\equiv \exp\left\{-a_i r_{12}^2 - b_i r_{13}^2 - c_i r_{14}^2 - d_i r_{23}^2 - e_i r_{24}^2 - f_i r_{34}^2\right\}. \end{aligned} \tag{118}$$

The first symmetry rule says we are free to, for example, exchange the positrons in the system. This amounts to swapping the indices $\{3 \leftrightarrow 4\}$ which gives the wave

function

$$\begin{aligned}\left|\psi_i^{1243}\right\rangle &\equiv \exp\left\{-a_i r_{12}^2 - b_i r_{14}^2 - c_i r_{13}^2 - d_i r_{24}^2 - e_i r_{23}^2 - f_i r_{34}^2\right\} \\ &= \phi\left(a_i, c_i, b_i, e_i, d_i, f_i\right).\end{aligned}$$

It turns out that if we exhaust all such symmetries then we find our wave function must be built up from eight such pieces (see Figure 4).

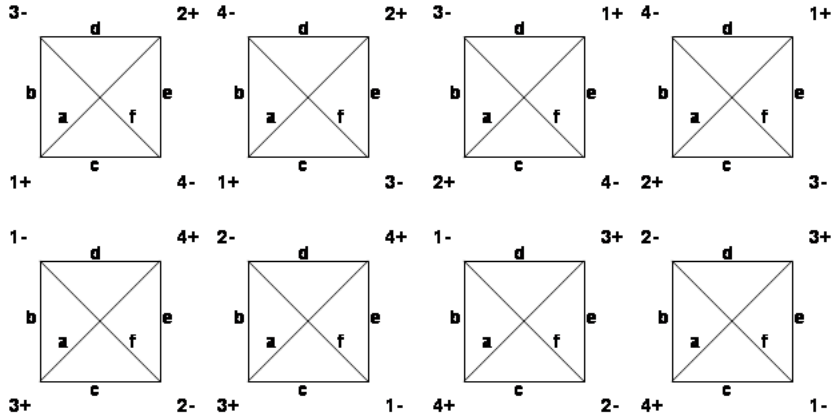


Figure 4: Physically equivalent configurations of the di-positronium system.

Thus the total trial wave function is

$$\begin{aligned}|\psi_i\rangle &= \left|\psi_i^{1234}\right\rangle + \left|\psi_i^{1243}\right\rangle + \left|\psi_i^{2134}\right\rangle + \left|\psi_i^{2143}\right\rangle \\ &\quad + \left|\psi_i^{3412}\right\rangle + \left|\psi_i^{3421}\right\rangle + \left|\psi_i^{4312}\right\rangle + \left|\psi_i^{4321}\right\rangle \\ &= \phi\left(a_i, b_i, c_i, d_i, e_i, f_i\right) + \phi\left(a_i, c_i, b_i, e_i, d_i, f_i\right) + \phi\left(a_i, d_i, e_i, b_i, c_i, f_i\right) \\ &\quad + \phi\left(a_i, e_i, d_i, c_i, b_i, f_i\right) + \phi\left(f_i, b_i, d_i, c_i, e_i, a_i\right) + \phi\left(f_i, c_i, e_i, b_i, d_i, a_i\right) \\ &\quad + \phi\left(f_i, d_i, b_i, e_i, c_i, a_i\right) + \phi\left(f_i, e_i, c_i, d_i, b_i, a_i\right). \qquad (119)\end{aligned}$$

The parameters $\{a_i, b_i, c_i, d_i, e_i, f_i; i = 0..(N-1)\}$ will be fine-tuned later during the optimization process in order to improve the upper bound on the eigenenergy. Since we would like to compare results from the effective field theory with those from the true theory we will need to calculate $\langle\psi_i|\psi_j\rangle$, $\langle\psi_i|\hat{H}|\psi_j\rangle$, and $\langle\psi_i|\hat{H}^{\Lambda}|\psi_j\rangle$ and solve the matrix problem in both cases. With each wave function broken up into the eight pieces as in equation (119) the resulting matrix elements will have 64 terms each (not including the fact that the Hamiltonians themselves are broken up into multiple pieces). To simplify this process we will for now consider only the matrix elements $\left\langle\psi_i^{1234}|\psi_j^{1234}\right\rangle$, $\left\langle\psi_i^{1234}\right|\hat{H}\left|\psi_j^{1234}\right\rangle$, and $\left\langle\psi_i^{1234}\right|\hat{H}^{\Lambda}\left|\psi_j^{1234}\right\rangle$ and then later on we can swap parameters in the resulting expressions to obtain the full set of matrix elements.

It will be advantageous later to have an expression for $\hat{T}\left|\psi_i^{1234}\right\rangle$ so let us work that out now before we move on. We will use the form of the kinetic energy operator $\hat{T}$ given by equation (114) in terms of gradients with respect to interparticle displacements. Taking gradients of the trial function (118) with respect to $\vec{r}_{12}$, $\vec{r}_{13}$, and $\vec{r}_{14}$ we can show

$$
\begin{aligned}
\nabla_{\vec{r}_{12}} |\psi\rangle &= \left[-2\left(a+d+e\right)\vec{r}_{12} + 2d\vec{r}_{13} + 2e\vec{r}_{14}\right] |\psi\rangle \,, \\
\nabla_{\vec{r}_{13}} |\psi\rangle &= \left[2d\vec{r}_{12} - 2\left(b+d+f\right)\vec{r}_{13} + 2f\vec{r}_{14}\right] |\psi\rangle \,, \\
\nabla_{\vec{r}_{14}} |\psi\rangle &= \left[2e\vec{r}_{12} + 2f\vec{r}_{13} - 2\left(c+e+f\right)\vec{r}_{14}\right] |\psi\rangle \,,
\end{aligned}
$$

where we have temporarily dropped the wave function and parameter indices. Taking a second gradient gives the various combinations needed to complete the kinetic energy operator,

$$
\begin{aligned}
\nabla^2_{\vec{r}_{12}} |\psi\rangle &= \Big[-6\left(a+d+e\right) + 4\Big[\left(a+d+e\right)^2 r_{12}^2 + d^2 r_{13}^2 + e^2 r_{14}^2 \\
&\quad -2d\left(a+d+e\right)\vec{r}_{12}\cdot\vec{r}_{13} - 2e\left(a+d+e\right)\vec{r}_{12}\cdot\vec{r}_{14} \\
&\quad +2de\vec{r}_{13}\cdot\vec{r}_{14}\Big]\Big] |\psi\rangle \,,
\end{aligned}
$$

$$
\begin{aligned}
\nabla^2_{\vec{r}_{13}} |\psi\rangle &= \Big[-6\left(b+d+f\right) + 4\Big[d^2 r_{12}^2 + \left(b+d+f\right)^2 r_{13}^2 + f^2 r_{14}^2 \\
&\quad -2d\left(b+d+f\right)\vec{r}_{12}\cdot\vec{r}_{13} + 2df\vec{r}_{12}\cdot\vec{r}_{14} \\
&\quad -2f\left(b+d+f\right)\vec{r}_{13}\cdot\vec{r}_{14}\Big]\Big] |\psi\rangle \,,
\end{aligned}
$$

$$
\begin{aligned}
\nabla^2_{\vec{r}_{14}} |\psi\rangle &= \Big[-6\left(c+e+f\right) + 4\Big[e^2 r_{12}^2 + f^2 r_{13}^2 + \left(c+e+f\right)^2 r_{14}^2 \\
&\quad +2ef\vec{r}_{12}\cdot\vec{r}_{13} - 2e\left(c+e+f\right)\vec{r}_{12}\cdot\vec{r}_{14} \\
&\quad -2f\left(c+e+f\right)\vec{r}_{13}\cdot\vec{r}_{14}\Big]\Big] |\psi\rangle \,,
\end{aligned}
$$

$$
\begin{aligned}
\nabla_{\vec{r}_{12}}\cdot\nabla_{\vec{r}_{13}} |\psi\rangle &= \Big[6d + 4\Big[-d\left(a+d+e\right) r_{12}^2 - d\left(b+d+f\right) r_{13}^2 + ef r_{14}^2 \\
&\quad + \left(d^2 + \left(a+d+e\right)\left(b+d+f\right)\right)\vec{r}_{12}\cdot\vec{r}_{13} \\
&\quad + \left(de - f\left(a+d+e\right)\right)\vec{r}_{12}\cdot\vec{r}_{14} \\
&\quad + \left(df - e\left(b+d+f\right)\right)\vec{r}_{13}\cdot\vec{r}_{14}\Big]\Big] |\psi\rangle \,,
\end{aligned}
$$

$$
\begin{aligned}
\nabla_{\vec{r}_{12}}\cdot\nabla_{\vec{r}_{14}} |\psi\rangle &= \Big[6e + 4\Big[-e\left(a+d+e\right) r_{12}^2 + df r_{13}^2 - e\left(c+e+f\right) r_{14}^2 \\
&\quad + \left(de - f\left(a+d+e\right)\right)\vec{r}_{12}\cdot\vec{r}_{13} \\
&\quad + \left(e^2 + \left(a+d+e\right)\left(c+e+f\right)\right)\vec{r}_{12}\cdot\vec{r}_{14} \\
&\quad + \left(ef - d\left(c+e+f\right)\right)\vec{r}_{13}\cdot\vec{r}_{14}\Big]\Big] |\psi\rangle \,,
\end{aligned}
$$

$$
\begin{aligned}
\nabla_{\vec{r}_{13}}\cdot\nabla_{\vec{r}_{14}} |\psi\rangle &= \Big[6d + 4\Big[der_{12}^2 - f\left(b+d+f\right) r_{13}^2 - f\left(c+e+f\right) r_{14}^2 \\
&\quad + \left(df - e\left(b+d+f\right)\right)\vec{r}_{12}\cdot\vec{r}_{13} \\
&\quad + \left(ef - d\left(c+e+f\right)\right)\vec{r}_{12}\cdot\vec{r}_{14} \\
&\quad + \left(f^2 + \left(b+d+f\right)\left(c+e+f\right)\right)\vec{r}_{13}\cdot\vec{r}_{14}\Big]\Big] |\psi\rangle \,.
\end{aligned}
$$

Adding these up and using the identity $2\vec{r}_{12}\cdot\vec{r}_{13} = r_{12}^2 + r_{13}^2 - r_{23}^2$ (law of cosines), we find

$$\begin{aligned}
\hat{T}\left|\psi\right\rangle &= [6\left(a+b+c+d+e+f\right) \\
&\quad -2\left(2a^2+ab+ad-bd+ac+ae-ce\right)r_{12}^2 \\
&\quad -2\left(2b^2+ab+bd-ad+bc+bf-cf\right)r_{13}^2 \\
&\quad -2\left(2c^2+ac+ce-ae+bc+cf-bf\right)r_{14}^2 \\
&\quad -2\left(2d^2+ad+bd-ab+de+df-ef\right)r_{23}^2 \\
&\quad -2\left(2e^2+ae+ce-ae+de+ef-df\right)r_{24}^2 \\
&\quad -2\left(2f^2+bf+cf-bc+df+ef-de\right)r_{34}^2]\left|\psi\right\rangle .
\end{aligned}$$

This allows us to break up the matrix element for the kinetic energy operator as

$$\begin{aligned}
\left\langle\psi_i^{1234}\right|\hat{T}\left|\psi_j^{1234}\right\rangle &= 6\left(a_i+b_i+c_i+d_i+e_i+f_i\right)\left\langle\psi_i^{1234}|\psi_j^{1234}\right\rangle \\
&\quad -2\left(2a_i^2+a_ib_i+a_id_i-b_id_i+a_ic_i+a_ie_i-c_ie_i\right)\left\langle r_{12}^2\right\rangle \\
&\quad -2\left(2b_i^2+a_ib_i+b_id_i-a_id_i+b_ic_i+b_if_i-c_if_i\right)\left\langle r_{13}^2\right\rangle \\
&\quad -2\left(2c_i^2+a_ic_i+c_ie_i-a_ie_i+b_ic_i+c_if_i-b_if_i\right)\left\langle r_{14}^2\right\rangle \\
&\quad -2\left(2d_i^2+a_id_i+b_id_i-a_ib_i+d_ie_i+d_if_i-e_if_i\right)\left\langle r_{23}^2\right\rangle \\
&\quad -2\left(2e_i^2+a_ie_i+c_ie_i-a_ie_i+d_ie_i+e_if_i-d_if_i\right)\left\langle r_{24}^2\right\rangle \\
&\quad -2\left(2f_i^2+b_if_i+c_if_i-b_ic_i+d_if_i+e_if_i-d_ie_i\right)\left\langle r_{34}^2\right\rangle ,
\end{aligned} \tag{120}$$

where $\left\langle r_{kl}^2\right\rangle \equiv \left\langle\psi_i^{1234}\right| r_{kl}^2 \left|\psi_j^{1234}\right\rangle$ and we have restored indices.

In order to determine the matrix elements for the exact potential we will need to find

$$\begin{aligned}
\left\langle\psi_i^{1234}\right|\hat{V}\left|\psi_j^{1234}\right\rangle &= \left\langle\psi_i^{1234}\right|\frac{1}{r_{12}}\left|\psi_j^{1234}\right\rangle + \left\langle\psi_i^{1234}\right|\frac{1}{r_{34}}\left|\psi_j^{1234}\right\rangle \\
&\quad -\left\langle\psi_i^{1234}\right|\frac{1}{r_{13}}\left|\psi_j^{1234}\right\rangle - \left\langle\psi_i^{1234}\right|\frac{1}{r_{14}}\left|\psi_j^{1234}\right\rangle \\
&\quad -\left\langle\psi_i^{1234}\right|\frac{1}{r_{23}}\left|\psi_j^{1234}\right\rangle - \left\langle\psi_i^{1234}\right|\frac{1}{r_{24}}\left|\psi_j^{1234}\right\rangle .
\end{aligned}$$

The cutoff potential is, of course, also broken up into six parts

$$\begin{aligned}
\left\langle \psi_i^{1234} \right| \hat{V}^{\Lambda} \left| \psi_j^{1234} \right\rangle &= \left\langle \psi_i^{1234} \right| \frac{1}{r_{12}} \mathrm{erf}\left( \frac{\Lambda r_{12}}{\sqrt{2}} \right) \left| \psi_j^{1234} \right\rangle \\
&+ \left\langle \psi_i^{1234} \right| \frac{1}{r_{34}} \mathrm{erf}\left( \frac{\Lambda r_{34}}{\sqrt{2}} \right) \left| \psi_j^{1234} \right\rangle \\
&- \left\langle \psi_i^{1234} \right| \frac{1}{r_{13}} \mathrm{erf}\left( \frac{\Lambda r_{13}}{\sqrt{2}} \right) \left| \psi_j^{1234} \right\rangle \\
&- \left\langle \psi_i^{1234} \right| \frac{1}{r_{14}} \mathrm{erf}\left( \frac{\Lambda r_{14}}{\sqrt{2}} \right) \left| \psi_j^{1234} \right\rangle \\
&- \left\langle \psi_i^{1234} \right| \frac{1}{r_{23}} \mathrm{erf}\left( \frac{\Lambda r_{23}}{\sqrt{2}} \right) \left| \psi_j^{1234} \right\rangle \\
&- \left\langle \psi_i^{1234} \right| \frac{1}{r_{24}} \mathrm{erf}\left( \frac{\Lambda r_{24}}{\sqrt{2}} \right) \left| \psi_j^{1234} \right\rangle , \qquad (121)
\end{aligned}$$

and finally the correction terms

$$\begin{aligned}
\left\langle \psi_i^{1234} \right| \hat{C}^{\Lambda} \left| \psi_j^{1234} \right\rangle &= \frac{\Lambda}{\sqrt{2\pi}} \left( 1 + \frac{5}{3\sqrt{\pi}\Lambda} \right) \\
&\times \left[ \left\langle \psi_i^{1234} \right| \exp\left( \frac{-\Lambda^2 r_{12}^2}{2} \right) \left| \psi_j^{1234} \right\rangle \right. \\
&+ \left\langle \psi_i^{1234} \right| \exp\left( \frac{-\Lambda^2 r_{34}^2}{2} \right) \left| \psi_j^{1234} \right\rangle \\
&- \left\langle \psi_i^{1234} \right| \exp\left( \frac{-\Lambda^2 r_{13}^2}{2} \right) \left| \psi_j^{1234} \right\rangle \\
&- \left\langle \psi_i^{1234} \right| \exp\left( \frac{-\Lambda^2 r_{14}^2}{2} \right) \left| \psi_j^{1234} \right\rangle \\
&- \left\langle \psi_i^{1234} \right| \exp\left( \frac{-\Lambda^2 r_{23}^2}{2} \right) \left| \psi_j^{1234} \right\rangle \\
&- \left. \left\langle \psi_i^{1234} \right| \exp\left( \frac{-\Lambda^2 r_{24}^2}{2} \right) \left| \psi_j^{1234} \right\rangle \right] . \qquad (122)
\end{aligned}$$

Let us also look at the two-particle contact densities as a test of the convergence of expectation values calculated with wave functions from each theory. After taking into account the symmetries of the system there are only two such operators to consider: the electron-positron contact density $\delta^3(\vec{r}_{14})$ and the positron-positron contact density (equivalent to electron-electron) $\delta^3(\vec{r}_{34})$. Thus we will also need to calculate

$$\left\langle \delta^3(\vec{r}_{14}) \right\rangle = \left\langle \psi_i^{1234} \right| \delta^3(\vec{r}_{14}) \left| \psi_j^{1234} \right\rangle , \qquad (123)$$

and

$$\left\langle \delta^3(\vec{r}_{13}) \right\rangle = \left\langle \psi_i^{1234} \right| \delta^3(\vec{r}_{34}) \left| \psi_j^{1234} \right\rangle . \qquad (124)$$

It remains now to perform the integrations that will give analytic forms for the matrix elements in terms of the parameters.

### 5.3 Coordinate Shift Approach for Gaussian Integrals

To begin let us consider the overlap integral

$$\langle\chi_i|\chi_j\rangle \;=\; \int \mathrm{d}^3\vec{A}_1\mathrm{d}^3\vec{A}_2\mathrm{d}^3\vec{A}_3\mathrm{d}^3\vec{A}_4\, e^{-ar_{12}^2-br_{13}^2-cr_{14}^2-dr_{23}^2-er_{24}^2-fr_{34}^2} \tag{125}$$

where $a = a_i + a_j$, $b = b_i + b_j$, etc., when $|\chi_i\rangle = \left|\psi_i^{1234}\right\rangle$ and $|\chi_j\rangle = \left|\psi_j^{1234}\right\rangle$. The full matrix elements can be obtained from this integral by changing the definitions of these parameters. The vectors $\vec{A}_i$ are the absolute coordinates of the particles as seen from the lab frame. The integration measure in (125) is the most general possible covering all possible positions of the four particles over all space. We actually only need to integrate over all possible configurations and we can disregard the position and motion of the center-of-mass in space since this has no physical implications without any external potentials.

First let us move to centre-of-mass coordinates defined by $\vec{A}_i = \vec{R} + \vec{R}_i$ and $\vec{R} = \frac{1}{4}\left(\vec{A}_1 + \vec{A}_2 + \vec{A}_3 + \vec{A}_4\right)$. It is straightforward to compute the Jacobian for this transformation

$$\frac{\partial\left(\vec{A}_1, \vec{A}_2, \vec{A}_3, \vec{A}_4\right)}{\partial\left(\vec{R}_1, \vec{R}_2, \vec{R}_3, \vec{R}\right)} = 4^3. \tag{126}$$

In centre-of-mass coordinates then our volume element becomes

$$4^3\mathrm{d}^3\vec{R}_1\mathrm{d}^3\vec{R}_2\mathrm{d}^3\vec{R}_3. \tag{127}$$

We have omitted integration over $\mathrm{d}^3\vec{R}$ since the trial wave function does not depend on the center-of-mass coordinate $\vec{R}$ and the resulting divergent integral will be canceled out upon normalization.

Moving next to relative coordinates defined by $\vec{r}_{ij} = \vec{R}_j - \vec{R}_i$ one can show the Jacobian of this transformation to be

$$\frac{\partial\left(\vec{R}_1, \vec{R}_2, \vec{R}_3\right)}{\partial\left(\vec{r}_{12}, \vec{r}_{13}, \vec{r}_{14}\right)} = 4^{-3}. \tag{128}$$

We can now rewrite the overlap integral with an integration measure suitable to the integrand as

$$\langle\chi_i|\chi_j\rangle \;\equiv\; I\left(a, b, c, d, e, f\right) \tag{129}$$

$$\;=\; \int \mathrm{d}^3\vec{r}_{12}\mathrm{d}^3\vec{r}_{13}\mathrm{d}^3\vec{r}_{14}\, e^{-ar_{12}^2-br_{13}^2-cr_{14}^2-dr_{23}^2-er_{24}^2-fr_{34}^2}. \tag{130}$$

In order to evaluate this integral first consider the coordinate shift

$$\begin{aligned}
\vec{r}_{12} &= \vec{x} + m_1\vec{y} + m_2\vec{z}, \\
\vec{r}_{13} &= \vec{y} + m_3\vec{z}, \\
\vec{r}_{14} &= \vec{z},
\end{aligned} \tag{131}$$

with unit Jacobian. The constants $m_1$, $m_2$, and $m_3$ will be determined later on. It follows from these definitions that

$$\begin{aligned}
\vec{r}_{23} &= \vec{r}_{13} - \vec{r}_{12} = -\vec{x} + (1 - m_1)\vec{y} + (m_3 - m_2)\vec{z}, \\
\vec{r}_{24} &= \vec{r}_{14} - \vec{r}_{12} = -\vec{x} - m_1\vec{y} + (1 - m_2)\vec{z}, \\
\vec{r}_{34} &= \vec{r}_{14} - \vec{r}_{13} = -\vec{y} + (1 - m_3)\vec{z}.
\end{aligned}$$

The argument of the exponential in (130) in the new coordinate system becomes

$$\begin{aligned}
-ar_{12}^2 - ... - fr_{34}^2 &= -a\left[x^2 + m_1^2 y^2 + m_2^2 z^2 + 2m_1 \vec{x}\cdot\vec{y}\right. \\
&\quad \left. + 2m_2 \vec{x}\cdot\vec{z} + 2m_1 m_2 \vec{y}\cdot\vec{z}\right] \\
&\quad -b\left[y^2 + m_3^2 z^2 + 2m_3 \vec{y}\cdot\vec{z}\right] - c\left[z^2\right] \\
&\quad -d\left[x^2 + (1 - m_1)^2 y^2 + (m_3 - m_2)^2 z^2\right. \\
&\quad \left. -2(1 - m_1)\vec{x}\cdot\vec{y} - 2(m_3 - m_2)\vec{x}\cdot\vec{z}\right. \\
&\quad \left. + 2(1 - m_1)(m_3 - m_2)\vec{y}\cdot\vec{z}\right] \\
&\quad -e\left[x^2 + m_1^2 y^2 + (1 - m_2)^2 z^2 + 2m_1 \vec{x}\cdot\vec{y}\right] \\
&\quad \left. -2(1 - m_2)\vec{x}\cdot\vec{z} - 2m_1(1 - m_2)\vec{y}\cdot\vec{z}\right] \\
&\quad -f\left[y^2 + (1 - m_3)^2 z^2 - 2(1 - m_3)\vec{y}\cdot\vec{z}\right]. \qquad (132)
\end{aligned}$$

Let us introduce a redundant set of parameters $m_4 = 1 - m_2$, $m_5 = 1 - m_3$. At first it looks like we have complicated things but we are now free to choose our parameters $m_1$, $m_4$, and $m_5$ so that all coefficients of the dot products in our new coordinates vanish. In order to make this determination we must solve for arbitrary $\vec{x}, \vec{y}, \vec{z}$ the set of equations

$$\begin{aligned}
(\vec{x}\cdot\vec{y})\left[am_1 - d(1 - m_1) + em_1\right] &= 0, \qquad (133) \\
(\vec{x}\cdot\vec{z})\left[a(1 - m_4) - d(m_4 - m_5) - em_4\right] &= 0, \qquad (134) \\
(\vec{y}\cdot\vec{z})\left[am_1(1 - m_4) + b(1 - m_5) + d(1 - m_1)(m_4 - m_5)\right. & \\
\left. -em_1 m_4 - fm_5\right] &= 0. \qquad (135)
\end{aligned}$$

Equation (133) tells us that

$$m_1 = \frac{d}{a + d + e}, \qquad (136)$$

and equation (134) gives us the relation

$$m_4 = 1 - m_2 = m_1\left(m_5 + \frac{a}{d}\right), \qquad (137)$$

which upon substituting into equation (135) gives

$$m_5 = 1 - m_3 = \frac{am_1 + b}{b + d + f - dm_1}. \qquad (138)$$

All of our coefficients are now fully determined and with these choices of parameters (132) can be rewritten

$$\begin{aligned}
-ar_{12}^2 - ... - fr_{34}^2 &= -a\left[x^2 + m_1^2 y^2 + m_2^2 z^2\right] - b\left[y^2 + m_3^2 z^2\right] - c\left[z^2\right] \\
&\quad -d\left[x^2 + (1-m_1)^2 y^2 + (m_3 - m_2)^2 z^2\right] \\
&\quad -e\left[x^2 + m_1^2 y^2 + (1-m_1)^2 z^2\right] \\
&\quad -f\left[y^2 + (1-m_3)^2 z^2\right] \\
&= -x^2\left[a + d + e\right] - y^2\left[a m_1^2 + b + d(1-m_1)^2 + e m_1^2 + f\right] \\
&\quad -z^2\left[a m_2^2 + b m_3^2 + c + d(m_3 - m_2)^2\right. \\
&\quad \left. +e(1-m_2)^2 + f(1-m_3)^2\right] \qquad (139) \\
&\equiv -\alpha_x x^2 - \alpha_y y^2 - \alpha_z z^2, \qquad (140)
\end{aligned}$$

where we have introduced the coefficients $\alpha_x$, $\alpha_y$, and $\alpha_z$ such that

$$\begin{aligned}
\alpha_x &= a + d + e\,, \\
\alpha_y &= \frac{(a+d+e)(b+d+f) - d^2}{a+d+e} = \frac{F_2(a,b,c,d,e,f)}{\alpha_x}\,, \\
\alpha_z &= \frac{F_1(a,b,c,d,e,f)}{(a+d+e)(b+d+f) - d^2} \\
&= \frac{F_1(a,b,c,d,e,f)}{\alpha_x \alpha_y} = \frac{F_1(a,b,c,d,e,f)}{F_2(a,b,c,d,e,f)},
\end{aligned}$$

with

$$\begin{aligned}
F_1(a,b,c,d,e,f) &\equiv abc + abe + abf + acd + acf + ade + adf + aef \\
&\quad +bcd + bce + bde + bdf + bef + cde + cdf + cef,
\end{aligned}$$

and

$$\begin{aligned}
F_2(a,b,c,d,e,f) &\equiv (a+d+e)(b+d+f) - d^2 \\
&= ab + ad + af + bd + be + de + df + ef.
\end{aligned}$$

The function $F_2$ will be useful later on when calculating matrix elements for the kinetic energy and potential parts of the Hamiltonian.

**Overlap Matrix Elements**

In this coordinate system it is straightforward to work out the overlap integral, equation (130),

$$I(\alpha_x, \alpha_y, \alpha_z) = \int \mathrm{d}^3\vec{x}\mathrm{d}^3\vec{y}\mathrm{d}^3\vec{z}\, e^{-\alpha_x x^2 - \alpha_y y^2 - \alpha_z z^2}, \qquad (141)$$

which can be integrated trivially to obtain

$$I(\alpha_x, \alpha_y, \alpha_z) = \frac{\pi^{9/2}}{(\alpha_x \alpha_y \alpha_z)^{3/2}}, \tag{142}$$

so that

$$I(\alpha_x, \alpha_y, \alpha_z) = \frac{\pi^{9/2}}{F_1(a,b,c,d,e,f)^{3/2}}. \tag{143}$$

Here we have found only one piece of the overlap matrix element, that for $|\chi_i\rangle = \left|\psi_i^{1234}\right\rangle$ and $|\chi_j\rangle = \left|\psi_j^{1234}\right\rangle$. The full overlap matrix element requires adding up 64 such pieces as discussed in §5.2 above. However, all of these pieces can be determined from this result, equation (143), by redefining the parameters $\{a, b, c, d, e, f\}$ according to the symmetries of the wave function in equation (119).

### Exact Coulomb Potential Matrix Elements

It turns out that we can work out all of the other matrix elements that we will need with simple modifications of the above integration. Let us next find the matrix elements for the exact Coulomb potential terms. Given the choice of coordinates (131) we can directly solve the integral

$$\begin{aligned} V_{14}(a,b,c,d,e,f) \equiv & \int \mathrm{d}^3\vec{r}_{12}\mathrm{d}^3\vec{r}_{13}\mathrm{d}^3\vec{r}_{14}\left(\frac{1}{r_{14}}\right) \\ & \times e^{-ar_{12}^2 - br_{13}^2 - cr_{14}^2 - dr_{23}^2 - er_{24}^2 - fr_{34}^2}, \end{aligned} \tag{144}$$

which transforms simply to

$$V_{14}(\alpha_x, \alpha_y, \alpha_z) = \int \mathrm{d}^3\vec{x}\mathrm{d}^3\vec{y}\mathrm{d}^3\vec{z}\left(\frac{1}{z}\right) e^{-\alpha_x x^2 - \alpha_y y^2 - \alpha_z z^2} \tag{145}$$

$$= \frac{\pi^3}{(\alpha_x\alpha_y)^{3/2}} \int \mathrm{d}^3\vec{z}\left(\frac{1}{z}\right) e^{-\alpha_z z^2} \tag{146}$$

$$= \frac{4\pi^4}{(\alpha_x\alpha_y)^{3/2}} \int_0^\infty \mathrm{d}z\, z\, e^{-\alpha_z z^2} \tag{147}$$

$$= \frac{2\pi^4}{F_1(a,b,c,d,e,f)\left[F_2(a,b,c,d,e,f)\right]^{1/2}}. \tag{148}$$

Swapping parameters in this result we can easily work out the other exact Coulomb integrals. For example

$$
\begin{aligned}
V_{12}(\mathbf{a},b,\mathbf{c},\mathbf{d},e,\mathbf{f}) &= \int \mathrm{d}^3\vec{r}_{12}\mathrm{d}^3\vec{r}_{13}\mathrm{d}^3\vec{r}_{14}\left(\frac{1}{r_{12}}\right) && (149)\\
&\quad \times e^{-\mathbf{a}r_{12}^2-br_{13}^2-\mathbf{c}r_{14}^2-\mathbf{d}r_{23}^2-er_{24}^2-\mathbf{f}r_{34}^2} \\
&= \int \mathrm{d}^3\vec{r}_{14}\mathrm{d}^3\vec{r}_{13}\mathrm{d}^3\vec{r}_{12}\left(\frac{1}{r_{12}}\right) && (150)\\
&\quad \times e^{-\mathbf{c}r_{14}^2-br_{13}^2-\mathbf{a}r_{12}^2-\mathbf{f}r_{34}^2-er_{24}^2-\mathbf{d}r_{23}^2} \\
&= \int \mathrm{d}^3\vec{r}_{12}\mathrm{d}^3\vec{r}_{13}\mathrm{d}^3\vec{r}_{14}\left(\frac{1}{r_{14}}\right) && (151)\\
&\quad \times e^{-\mathbf{c}r_{12}^2-br_{13}^2-\mathbf{a}r_{14}^2-\mathbf{f}r_{23}^2-er_{24}^2-\mathbf{d}r_{34}^2} \\
&\equiv V_{14}(\mathbf{c},b,\mathbf{a},\mathbf{f},e,\mathbf{d}). && (152)
\end{aligned}
$$

From line (149) to (150) we simply rearrange the integral so that $\vec{r}_{12}$ takes the role of $\vec{r}_{14}$ in equation (144). Then to get to (151) we simply change the indices (in this case swapping $2 \leftrightarrow 4$) and the result is an integral equivalent to the one we already know. Similarily, one can show

$$
\begin{aligned}
V_{13}(a,\mathbf{b},\mathbf{c},\mathbf{d},\mathbf{e},f) &= V_{14}(a,\mathbf{c},\mathbf{b},\mathbf{e},\mathbf{d},f), && (153)\\
V_{23}(a,\mathbf{b},\mathbf{c},\mathbf{d},\mathbf{e},f) &= V_{14}(a,\mathbf{e},\mathbf{d},\mathbf{c},\mathbf{b},f), && (154)\\
V_{24}(a,\mathbf{b},\mathbf{c},\mathbf{d},\mathbf{e},f) &= V_{14}(a,\mathbf{d},\mathbf{e},\mathbf{b},\mathbf{c},f), && (155)\\
V_{34}(\mathbf{a},\mathbf{b},\mathbf{c},\mathbf{d},\mathbf{e},\mathbf{f}) &= V_{14}(\mathbf{b},\mathbf{d},\mathbf{f},\mathbf{a},\mathbf{c},\mathbf{e}). && (156)
\end{aligned}
$$

As with the overlap integral, we have only been using one part of the wave function so this result does not give us the full matrix element. The next step is adjust the parameters in equations (148,152-156) so as to account for all of the symmetries discussed in §5.2 and add up the resulting matrix elements.

**Effective Potential Matrix Elements**

Next we evaluate the cutoff potential matrix elements, one of which is

$$
\begin{aligned}
V_{14}^{\Lambda}(a,b,c,d,e,f) &\equiv \int \mathrm{d}^3\vec{r}_{12}\mathrm{d}^3\vec{r}_{13}\mathrm{d}^3\vec{r}_{14}\left(\frac{1}{r_{14}}\mathrm{erf}\left\{\frac{\Lambda}{\sqrt{2}}r_{14}\right\}\right) \\
&\quad \times e^{-ar_{12}^2-br_{13}^2-cr_{14}^2-dr_{23}^2-er_{24}^2-fr_{34}^2}.
\end{aligned}
$$

Under the coordinate transformation (131) this gives

$$
\begin{aligned}
V_{14}^{\Lambda}(a,b,c,d,e,f) &= \int \mathrm{d}^3\vec{x}\mathrm{d}^3\vec{y}\mathrm{d}^3\vec{z}\left(\frac{1}{z}\mathrm{erf}\left\{\frac{\Lambda}{\sqrt{2}}z\right\}\right) \\
&\quad \times e^{-\alpha_x x^2-\alpha_y y^2-\alpha_z z^2} \\
&= \frac{\pi^3}{(\alpha_x\alpha_y)^{3/2}}\int \mathrm{d}^3\vec{z}\left(\frac{1}{z}\mathrm{erf}\left\{\frac{\Lambda}{\sqrt{2}}z\right\}\right)e^{-\alpha_z z^2} \\
&= \frac{4\pi^4}{(\alpha_x\alpha_y)^{3/2}}\int_0^\infty \mathrm{d}z\, z\,\mathrm{erf}\left\{\frac{\Lambda}{\sqrt{2}}z\right\}e^{-\alpha_z z^2} \\
&= \frac{2\pi^4}{F_1\sqrt{F_2+\frac{2\alpha^2 F_1}{\Lambda^2}}}. \qquad (157)
\end{aligned}
$$

Using the same tricks as in (149-152) it is straightforward to show

$$
\begin{aligned}
V_{12}^{\Lambda}(\mathbf{a},b,\mathbf{c},\mathbf{d},e,\mathbf{f}) &= V_{14}^{\Lambda}(\mathbf{c},b,\mathbf{a},\mathbf{f},e,\mathbf{d}), &(158)\\
V_{13}^{\Lambda}(a,\mathbf{b},\mathbf{c},\mathbf{d},\mathbf{e},f) &= V_{14}^{\Lambda}(a,\mathbf{c},\mathbf{b},\mathbf{e},\mathbf{d},f), &(159)\\
V_{23}^{\Lambda}(a,\mathbf{b},\mathbf{c},\mathbf{d},\mathbf{e},f) &= V_{14}^{\Lambda}(a,\mathbf{e},\mathbf{d},\mathbf{c},\mathbf{b},f), &(160)\\
V_{24}^{\Lambda}(a,\mathbf{b},\mathbf{c},\mathbf{d},\mathbf{e},f) &= V_{14}^{\Lambda}(a,\mathbf{d},\mathbf{e},\mathbf{b},\mathbf{c},f), &(161)\\
V_{34}^{\Lambda}(\mathbf{a},\mathbf{b},\mathbf{c},\mathbf{d},\mathbf{e},\mathbf{f}) &= V_{14}^{\Lambda}(\mathbf{b},\mathbf{d},\mathbf{f},\mathbf{a},\mathbf{c},\mathbf{e}). &(162)
\end{aligned}
$$

Again, we construct the full effective potential matrix element, as we did for the exact potential, by adding up terms of the form (157) for the various parameter choices that take into account all of the symmetries of the system.

**Effective Potential Correction Matrix Elements**

The matrix elements for the correction terms to the effective potential are given by evaluating integrals of the form

$$
\begin{aligned}
C_{14}^{\Lambda}(a,b,c,d,e,f) &\equiv \int \mathrm{d}^3\vec{r}_{12}\mathrm{d}^3\vec{r}_{13}\mathrm{d}^3\vec{r}_{14}\left(\exp\left\{-\frac{\Lambda^2}{2}r_{14}^2\right\}\right) \\
&\quad \times e^{-ar_{12}^2-br_{13}^2-cr_{14}^2-dr_{23}^2-er_{24}^2-fr_{34}^2} \\
&= \int \mathrm{d}^3\vec{r}_{12}\mathrm{d}^3\vec{r}_{13}\mathrm{d}^3\vec{r}_{14} \\
&\quad \times e^{-ar_{12}^2-br_{13}^2-\left(c+\frac{\Lambda^2}{2}\right)r_{14}^2-dr_{23}^2-er_{24}^2-fr_{34}^2} \\
&\equiv I(a,b,\left(c+\frac{\Lambda^2}{2}\right),d,e,f).
\end{aligned}
$$

In other words they are simply given by the overlap integral with a shift in the parameter corresponding to the scalar distance involved. In this manner we can show

$$C_{12}^{\Lambda}(\mathbf{a},b,c,d,e,f) = I(\left(\mathbf{a}+\frac{\mathbf{\Lambda^2}}{\mathbf{2}}\right),b,c,d,e,f), \quad (163)$$

$$C_{13}^{\Lambda}(a,\mathbf{b},c,d,e,f) = I(a,\left(\mathbf{b}+\frac{\mathbf{\Lambda^2}}{\mathbf{2}}\right),c,d,e,f), \quad (164)$$

$$C_{23}^{\Lambda}(a,b,c,\mathbf{d},e,f) = I(a,b,c,\left(\mathbf{d}+\frac{\mathbf{\Lambda^2}}{\mathbf{2}}\right),e,f), \quad (165)$$

$$C_{24}^{\Lambda}(a,b,c,d,\mathbf{e},f) = I(a,b,c,d,\left(\mathbf{e}+\frac{\mathbf{\Lambda^2}}{\mathbf{2}}\right),f), \quad (166)$$

$$C_{34}^{\Lambda}(a,b,c,d,e,\mathbf{f}) = I(a,b,c,d,e,\left(\mathbf{f}+\frac{\mathbf{\Lambda^2}}{\mathbf{2}}\right)). \quad (167)$$

To construct the matrix element for the full wave function we again need to sum up terms like these with parameters redefined to account for all of the symmetries of the system.

### Kinetic Energy Matrix Elements

Equation (120) tells us that in order to compute the matrix elements for the kinetic energy terms we will need the integral $I(a,b,c,d,e,f)$ as well as integrals of the form

$$T_{14}(a,b,c,d,e,f) \equiv \int \mathrm{d}^3\vec{r}_{12}\mathrm{d}^3\vec{r}_{13}\mathrm{d}^3\vec{r}_{14}\left(r_{14}^2\right) \times e^{-ar_{12}^2-br_{13}^2-cr_{14}^2-dr_{23}^2-er_{24}^2-fr_{34}^2},$$

which in the $(\vec{x},\vec{y},\vec{z})$ coordinate system becomes

$$T_{14}(a,b,c,d,e,f) = \int \mathrm{d}^3\vec{x}\mathrm{d}^3\vec{y}\mathrm{d}^3\vec{z}\left(z^2\right)e^{-\alpha_x x^2-\alpha_y y^2-\alpha_z z^2} \quad (168)$$

$$= \frac{\pi^3}{\left(\alpha_x\alpha_y\right)^{3/2}}\int \mathrm{d}^3\vec{z}\left(z^2\right)e^{-\alpha_z z^2} \quad (169)$$

$$= \frac{4\pi^4}{\left(\alpha_x\alpha_y\right)^{3/2}}\int_0^{\infty}\mathrm{d}z\, z^4 e^{-\alpha_z z^2} \quad (170)$$

$$= \frac{3\pi^{9/2}}{2\alpha_z\left(\alpha_x\alpha_y\alpha_z\right)^{3/2}} \quad (171)$$

$$= \frac{3\pi^{9/2}F_2\left(a,b,c,d,e,f\right)}{2\left[F_1\left(a,b,c,d,e,f\right)\right]^{5/2}}. \quad (172)$$

The other integrals for kinetic energy terms can be found again by swapping parameters. In particular

$$
\begin{aligned}
T_{12}(\mathbf{a},b,\mathbf{c},\mathbf{d},e,\mathbf{f}) &= T_{14}(\mathbf{c},b,\mathbf{a},\mathbf{f},e,\mathbf{d}), && (173)\\
T_{13}(a,\mathbf{b},\mathbf{c},\mathbf{d},\mathbf{e},f) &= T_{14}(a,\mathbf{c},\mathbf{b},\mathbf{e},\mathbf{d},f), && (174)\\
T_{23}(a,\mathbf{b},\mathbf{c},\mathbf{d},\mathbf{e},f) &= T_{14}(a,\mathbf{e},\mathbf{d},\mathbf{c},\mathbf{b},f), && (175)\\
T_{24}(a,\mathbf{b},\mathbf{c},\mathbf{d},\mathbf{e},f) &= T_{14}(a,\mathbf{d},\mathbf{e},\mathbf{b},\mathbf{c},f), && (176)\\
T_{34}(\mathbf{a},\mathbf{b},\mathbf{c},\mathbf{d},\mathbf{e},\mathbf{f}) &= T_{14}(\mathbf{b},\mathbf{d},\mathbf{f},\mathbf{a},\mathbf{c},\mathbf{e}). && (177)
\end{aligned}
$$

We can now compute the matrix element (120) since

$$
\begin{aligned}
\left\langle \psi_i^{1234}\right| \hat{T} \left|\psi_j^{1234}\right\rangle &= 6\left(a_j+b_j+c_j+d_j+e_j+f_j\right)\left\langle \psi_i^{1234}|\psi_j^{1234}\right\rangle\\
&\quad -2\left(2a_i^2+a_ib_i+a_id_i-b_id_i+a_ic_i+a_ie_i-c_ie_i\right)\left\langle r_{12}^2\right\rangle\\
&\quad -2\left(2b_i^2+a_ib_i+b_id_i-a_id_i+b_ic_i+b_if_i-c_if_i\right)\left\langle r_{13}^2\right\rangle\\
&\quad -2\left(2c_i^2+a_ic_i+c_ie_i-a_ie_i+b_ic_i+c_if_i-b_if_i\right)\left\langle r_{14}^2\right\rangle\\
&\quad -2\left(2d_i^2+a_id_i+b_id_i-a_ib_i+d_ie_i+d_if_i-e_if_i\right)\left\langle r_{23}^2\right\rangle\\
&\quad -2\left(2e_i^2+a_ie_i+c_ie_i-a_ie_i+d_ie_i+e_if_i-d_if_i\right)\left\langle r_{24}^2\right\rangle\\
&\quad -2\left(2f_i^2+b_if_i+c_if_i-b_ic_i+d_if_i+e_if_i-d_ie_i\right)\left\langle r_{34}^2\right\rangle,
\end{aligned}
$$

and we already have $\left\langle \psi_i^{1234}|\psi_j^{1234}\right\rangle$ from equation (143) above. Note that in the above notation, $\left\langle r_{13}^2\right\rangle = \left\langle \psi_i^{1234}\right| r_{13}^2 \left|\psi_j^{1234}\right\rangle = T_{13}(a_i+a_j,b_i+b_j,c_i+c_j,d_i+d_j,e_i+e_j,f_i+f_j)$, and so on. Then to construct the entire kinetic energy matrix element we add together 64 pieces like this with parameters chosen according to the symmetry rules outlined in §5.2.

### Delta Function Matrix Elements

Last, we come to the matrix elements for the electron-positron and positron-positron contact densities. Considering first the electron-positron contact density we have to compute

$$
\begin{aligned}
\left\langle \psi_i^{1234}\right| \delta\left(\vec{r}_{14}\right) \left|\psi_j^{1234}\right\rangle &\equiv \int \mathrm{d}^3\vec{r}_{12}\mathrm{d}^3\vec{r}_{13}\mathrm{d}^3\vec{r}_{14}\left(\delta\left(\vec{r}_{14}\right)\right)\\
&\qquad \times e^{-ar_{12}^2-br_{13}^2-cr_{14}^2-dr_{23}^2-er_{24}^2-fr_{34}^2}\\
&= \int \mathrm{d}^3\vec{r}_{12}\mathrm{d}^3\vec{r}_{13}\, e^{-(a+e)r_{12}^2-(b+f)r_{13}^2-dr_{23}^2}.
\end{aligned}
$$

This is just the overlap integral for the positronium-ion with $a \rightarrow (a+e)$ and $b \rightarrow (b+f)$. Thus, using the result in equation (60) we have

$$
\left\langle \psi_i^{1234}\right| \delta\left(\vec{r}_{14}\right) \left|\psi_j^{1234}\right\rangle = \frac{\pi^3}{\left(\left(a+e\right)\left(b+f\right)+\left(a+e\right)d+\left(b+f\right)d\right)^{3/2}}. \quad (178)
$$

Similarly, for the positron-positron contact density one can show

$$
\begin{aligned}
\left\langle \psi_i^{1234}\right| \delta\left(\vec{r}_{34}\right) \left|\psi_j^{1234}\right\rangle &= \int \mathrm{d}^3\vec{r}_{12}\mathrm{d}^3\vec{r}_{13}\, e^{-(d+e)r_{12}^2-(b+c)r_{13}^2-ar_{23}^2}\\
&= \frac{\pi^3}{\left(\left(d+e\right)\left(b+c\right)+\left(d+e\right)a+\left(b+c\right)a\right)^{3/2}}. \quad (179)
\end{aligned}
$$

Both of these matrix elements are again only a piece of the matrix elements for the full wave function. However, the full matrix elements can be found by simply swapping parameters around in (178) and (179) so as to exhaust all possible symmetries of the wave function.

### 5.4 Results

At this point we can use the matrix elements for the effective and exact Hamiltonians to find an optimal set of parameters $\{a_i, b_i, c_i, d_i, e_i, f_i; i = 0..(N-1)\}$ that minimize the di-positronium ground state energy. Let us first compare the bound state energies produced by each theory for difference basis sizes. For the effective field theory we take $\Lambda = 50$. Results for various size bases of trial wave functions are shown in Table 4.

| Basis Size ($N$) | EFT at $\mathcal{O}(\alpha)$, $\left\langle \hat{H}^{\Lambda} \right\rangle$ | Correction, $\left\langle \hat{C}^{\Lambda} \right\rangle$ | EFT at $\mathcal{O}(\alpha^3)$, $\left\langle \hat{H}^{\Lambda} \right\rangle + \left\langle \hat{C}^{\Lambda} \right\rangle$ | Exact Theory, $\left\langle \hat{H} \right\rangle$ |
|---|---|---|---|---|
| 10 | -0.51336375 | -0.00018141 | -0.51354516 | -0.51221924 |
| 20 | -0.51532713 | -0.00020120 | -0.51552833 | -0.51546153 |
| 40 | -0.51567711 | -0.00020871 | -0.51588582 | -0.51588625 |
| 60 | -0.51575941 | -0.00021130 | -0.51597071 | -0.51596430 |
| 80 | -0.51577822 | -0.00021212 | -0.51599034 | -0.51598202 |
| 100 | -0.51578340 | -0.00021217 | -0.51599557 | -0.51599207 |
| 120 | -0.51578378 | -0.00021222 | -0.51599600 | -0.51599325 |
| 160 | -0.51578850 | -0.00021242 | -0.51600093 | -0.51599945 |
| 200 | -0.51578936 | -0.00021250 | -0.51600186 | -0.51600070 |

Table 4: Ground state energy of the di-positronium molecule in units $m\alpha^2$.

Current estimates show the actual energy of the di-positronium molecule ground state to eight decimal places to be $-0.51600379\, m\alpha^2$ [8]. As we can see in Table 4: Columns 4 and 5 all of the energies produced by both the true theory and effective theory appear to be converging to this value and, more importantly, they do not drop below it. In both cases, as the basis grows to $N = 200$, our values differ from the true result by just a few parts in $10^6$. This agreement is not quite as good as that for the positronium-ion in §4 but this is to be expected because the wave function for the four-body di-positronium molecule is much more complicated. On the bright side, the effective field theory results here (Table 4: Column 4) do not overshoot the actual result as they did with the positronium-ion because at this precision the next order corrections ($\mathcal{O}(\alpha^4)$) do not come into play.

With regards to the rate of convergence of the two methods, the effective field theory seems to be very slightly better than the true theory. We can see this by noting that for $N = 40$ the two theories gives very close results but beyond that, for $N \geq 60$, the effective field theory is always lower, although by only a few parts in $10^6$. This should not be surprising, however, because our trial wave functions, which are Gaussians, are better suited to the smooth nature of the wave function of the effective field theory. However, a difference of only a few parts in $10^6$ in the energies does not give us any definite information on if the wave function for the effective

theory is converging to the true di-positronium wave function better than our wave function from the exact theory.

To determine which wave function is more useful we want to see which will give us expectation values that converge to their actual values faster. Once the optimization routine determines an energy estimate (those in Table 4) it also gives us the corresponding eigenvector and a tuned parameter set. From these two objects we can construct an approximate full wave function for the system and then calculate expectation values. Here we present the results of calculating expectation values for the electron-positron and positron-positron contact densities (Table 5). For comparison, we calculate them with both the effective field theory and exact theory approximate wave functions.

| Basis Size ($N$) | $\langle\delta_{e^+e^-}\rangle$ using EFT | $\langle\delta_{e^+e^-}\rangle$ using Exact Theory | $\langle\delta_{e^+e^+}\rangle$ using EFT | $\langle\delta_{e^+e^+}\rangle$ using Exact Theory |
|---|---|---|---|---|
| 10 | 0.018198 | 0.017264 | 0.00082408 | 0.00076688 |
| 20 | 0.020100 | 0.020091 | 0.00078380 | 0.00073796 |
| 40 | 0.020868 | 0.021109 | 0.00068294 | 0.00067055 |
| 60 | 0.021158 | 0.021478 | 0.00066185 | 0.00066208 |
| 80 | 0.021259 | 0.021676 | 0.00066322 | 0.00065517 |
| 100 | 0.021284 | 0.021681 | 0.00065051 | 0.00064643 |
| 120 | 0.021288 | 0.021769 | 0.00064917 | 0.00064400 |
| 160 | 0.021299 | 0.021874 | 0.00064881 | 0.00064287 |
| 200 | 0.021311 | 0.021890 | 0.00064621 | 0.00064082 |

Table 5: Expectation values of delta functions, $\delta_{e^+e^-}$ and $\delta_{e^+e^+}$, for di-positronium molecule.

For the di-positronium molecule the actual value for the electron-positron contact density is 0.022118 and for the positron-positron contact density it is 0.00062580 (each value given to five significant digits) [7]. As we can see in Table 5, all of the values are well behaved and appear to be moving in the right direction. However, as was the case with the positronium-ion, the expectation values of the electron-positron contact density for the effective field theory converge faster than those for the true theory but not to the right value (see Table 5: Column 2). The true theory, on the other hand, takes longer to settle on a particular value but seems to be closing in on the correct one (see Table 5: Column 3). For the positron-positron contact density expectation values (Table 5: Columns 4 and 5) both theories do a reasonable job, but the exact theory does slightly better. Thus, in each case the wave function from the effective field theory does not perform as well as that from the true theory. This is almost certainly due to the fact that the effective potential has no divergence at $\vec{r} = 0$ and in turn gives rises to a wave function that is smooth there. This makes the wave function unreliable for working out expectation values for the exact theory whose wave function has a cusp at $\vec{r} = 0$. The wave function produced using the true theory, on the other hand, better approximates the cusp and that is why it ultimately gives better results.

# 6 Conclusions

When attempting to determine the properties of a complicated quantum system, one cannot always hope to find an exact wave function. Often, the only way to proceed is to perform a variational calculation and try to approximate the wave function for the system. Usually, this also means performing a numerical calculation, especially if one wants to perform some sort of optimization of the wave function. However, as physicists try to determine the properties of increasingly complicated systems to higher and higher precisions, it becomes important to find shortcuts for these types of problems.

As we have seen, if one is interested in the low-energy phenomena associated with a system, it is straightforward to construct an effective field theory that mimics the true theory to arbitrarily high precision. Additionally, one can remove certain inconvenient features of the true theory (e.g. cusps, divergences). The wave function associated with the resulting effective field theory should consequently be much smoother than that of the true theory. This could be a great advantage if we are trying to approximate our wave function with a basis of smooth functions. When this is the case, which it often is, then we would expect an optimization routine to produce the wave function for the effective theory faster than it could that of the true theory. If this wave function could then lend itself to calculating accurate expectation values that converged faster than those calculated using the true theory, then this would be a great advantage of using effective field theories.

To test this idea we considered both the three-body positronium-ion and the four-body di-positronium molecule, each with the true theory (Coulomb) and an effective theory (Coulomb with high-energy cutoff). We then performed a variational calculation using multiple Gaussian trial wave functions with tunable parameters. Using these smooth Gaussians meant that we could accurately construct the wave function for the effective theory with fewer basis functions than we would need to do the same for the true theory. An optimization routine allowed us to seek out the parameters which gave a minimum upper bound on the energy of the system as well as an approximate wave function. We could then compare the effectiveness of the well-converged wave function from the effective theory with the slowly converging wave function from the true theory. This was done for multiple basis sizes so that convergence properties could be observed.

For the positronium-ion bound state energy, with a basis size $N = 240$, the optimized wave functions gave for the true theory $-0.262005057\, m\alpha^2$ and for the effective theory $-0.262005304\, m\alpha^2$ (the actual value to nine decimal places being $-0.262005070\, m\alpha^2$). As we can see, there is excellent agreement between the result from the true theory and the actual result, differing by less than two parts in $10^8$. Unfortunately, the lack of corrections beyond $\mathcal{O}\left(\alpha^3\right)$ in our effective theory resulted in an energy lower than the actual value. More important than the final precision, however, is how well the energies converged as the basis size increased. In both cases, the convergence is clear and, not surprisingly, the energies for the effective field theory converge faster. This is because we can construct the wave function for the effective theory much more easily with Gaussians than we can the wave function for the true theory. Nevertheless, the wave function from the effective theory has no advantage over the wave function from the true theory if it cannot be used to calculate expectation values that converge faster (and to the actual value) as well. To

test this we used the tuned wave functions to compute the electron-positron contact density for the positronium-ion. At the largest basis size of $N = 240$ the wave function from the true theory gave a value of 0.020671 very close to the actual value of 0.020733 (to five significant digits), while the wave function from the effective theory only gave 0.020029. More seriously, the effective theory results appeared to converge to this value very quickly and then did not change significantly, implying convergence to an incorrect final answer. This is another indication that the wave function from the effective theory converged very quickly but, unfortunately, it also means that it is not useful for practical applications.

Before we moved on from the positronium-ion, we took advantage of the fact that we were in possession of a highly-tuned wave function for that system to calculate a useful expectation value. We reasoned that the pair of electrons with no net magnetic moment could alter the magnetic moment of the positron, which characterizes the magnetic moment of the ion. This, we determined, would be an $\mathcal{O}\left(\alpha^2\right)$ correction. We then found that in order to calculate this correction for the positronium-ion one needed the expectation value of the scalar product of the electric field as felt by the positron with its center-of-mass position which has not been calculated to our knowledge. After finding an explicit formula for this expectation value in terms of our Gaussian basis trial functions, we then computed it using our tuned wave function and found the currently unknown matrix element to be

$$\left\langle \vec{\varepsilon} \cdot \vec{R} \right\rangle = -0.25753 \pm \left(1 \times 10^{-5}\right) m\alpha^{3/2}. \tag{180}$$

Our next system to test the potential benefits of using an effective field theory was the di-positronium molecule. For a basis size $N = 200$, the optimized wave functions found ground state energies for the true theory of $-0.51600070\, m\alpha^2$ and for the effective theory $-0.51600186\, m\alpha^2$ (the actual value to eight decimal places being $-0.51600379\, m\alpha^2$). Again we have very good agreement between the energy produced here by the true theory and the actual energy, differing by a few parts in $10^6$. This time, however, our effective theory produces an even closer result without going lower than the actual value, also differing by a few parts in $10^6$. The fact that we did not overshoot with the effective theory this time is to be expected since for the di-positronium molecule the program did not achieve precision that made the $\mathcal{O}\left(\alpha^4\right)$ correction important. It is also not surprising that neither method could match the precision achieved with the positronium-ion simply because the wave function for the molecule is much more complicated and, thus, not as easily constructed from our trial basis. The precision we obtained was not the main issue though. We were primarily concerned with how well the energies converged as the basis size increased. There is clear convergence again in both cases with the effective field theory converging faster again, but only slightly. To answer the convergence question more definitely we use the wave functions obtained to compute the positron-positron and electron-positron contact densities for the system. For the electron-positron contact density at the largest basis size of $N = 200$, the wave function from the true theory gave a value of 0.021890, which is quite close to the actual value of 0.022118 (to five significant digits) while the wave function from the effective theory came up shy again, giving only 0.021311. As was the case with the ion, the electron-positron contact density expectation value as predicted by the effective theory suffered from the defect of converging to the wrong value. For the positron-positron contact density at the

largest basis size, the wave function from the true theory gave a value of $6.4082 \times 10^{-4}$ while the wave function from the effective theory gave $6.4621 \times 10^{-4}$. The actual value (to five significant digits) is $6.2580 \times 10^{-4}$ so again the true theory did a better job.

For both systems of interest, the effective field theory and true theory were both able to produce very accurate energies. As expected, the energies from the effective theory always converged faster as well. This, we said, was because the wave function for the effective theory is easier to construct with a basis of smooth trial functions. However, when we went on to compare the effectiveness of the wave functions in calculating expectation values, the effective theory clearly fell short. The results from the effective theory still converged as fast or faster than the true theory but they were never as accurate in the end. However, the expectation value of the delta function is a particularly severe test of the effective theory, since it probes the wave function exactly at the place where the change of the potential affects it most strongly. It is likely that other operators can be evaluated more reliably with the effective theory. Even the delta function can be rewritten with the help of equations of motion in terms of operators that probe more global properties of the wave function [11]. A definite answer to this question will require more work since here, despite the fact that our energies and wave functions from the effective theory converged faster than their true theory counterparts, we did not see any obvious advantage to using an effective field theory, because its predictions ultimately did not match the reliability and accuracy of the true theory.

## References


[1] A. I. Akhiezer and V. B. Berestskii. *Quantum Electrodynamics*. Interscience Publ., New York, 1965.

[2] C. D. Anderson. *Phys. Rev.*, **43**:491–494, 1933.

[3] T. Aoyama, M. Hayakawa, T. Kinoshita, and M. Nio. *Phys. Rev. D*, **78**:113006, 2008.

[4] H. Bethe and E. Salpeter. *Quantum Mechanics of One- and Two-Electron Atoms*. Dover Publications, 1977.

[5] A. K. Bhatia and R. J. Drachman. *Phys. Rev. A*, **28**:2523–2525, 1983.

[6] G. Breit. *Phys. Rev. A*, **122**:649, 1928.

[7] S. Bubin and L. Adamowicz. *Phys. Rev. A*, **74**:052502, 2006.

[8] S. Bubin, M. Stanke, D. Kedziera, and L. Adamowicz. *Phys. Rev. A*, **75**:062504, 2007.

[9] M. Deutsch and E. Dulit. *Phys. Rev.*, **84**:601–602, 1951.

[10] P. Dirac. *Proc. R. Soc. Lond. A*, **117**:610–624, 1928.

[11] R. J. Drachman. *J. Phys. B*, **14**:2733, 1981.

[12] A. M. Frolov. *Phys. Rev. A*, **60**:2834, 1999.

[13] A. M. Frolov. *Phys. Rev. E*, **74**:027702, 2007.

[14] A. M. Frolov and D. H. Bailey. *Phys. Rev. A*, **72**:014501, 2005.

[15] A. M. Frolov and V. H. Smith Jr. *Phys. Rev. A*, **55**:2662, 1997.

[16] A. A. Frost, M. Inokuti, and J. P. Lowe. *J. Chem. Phys.*, **41**:482, 1964.

[17] G. H. Golub and C. F. Van Loan. *Matrix Computations*. The John Hopkins University Press, 1990.

[18] R. Hill. *AIP Conf. Proc., arXiv:hep-ph/0008002v1*, 2008.

[19] Y. K. Ho. *J. Phys. B.: At. Mol. Phys.*, **16**:1503–1509, 1982.

[20] Y. K. Ho. *Phys. Rev. A*, **33**:3584, 1986.

[21] E. A. Hylleraas. *Phys. Rev.*, **71**:491, 1947.

[22] E. A. Hylleraas and A. Ore. *Phys. Rev.*, **71**:493, 1947.

[23] A. P. Mills Jr. *Phys. Rev. Lett.*, **46**:717–720, 1980.

[24] A. P. Mills Jr. and D. B. Cassidy. *Nature*, **449**:195–197, 2007.

[25] S. G. Karshenboim. *Phys. Lett.*, **A266**:380, 2000.

[26] D. B. Kinghorn and R. D. Poshusta. *Phys. Rev. A*, **47**:3671, 1993.

[27] G. P. Lepage. *arXiv:nucl-th/9706029v1*, 1997.

[28] E. Merzbacher. *Quantum Mechanics*. John Wiley and Sons, Inc., 1998.

[29] S. Mohorovicic. *Astron. Nachr*, **253**:94, 1934.

[30] A. Ore. *Phys. Rev.*, **70**:90, 1993.

[31] A. A. Penin. *Int. J. Mod. Phys. A*, **19**:3897–3904, 2004.

[32] J. Pesonen and L. Halonen. *J. Chem. Phys.*, **116**:1825, 2001.

[33] W. H. Press, S. A. Teukolsky, W. T. Vetterling, and B. P. Flannery. *Numerical Recipes: The Art of Scientific Computation*. Cambridge University Press, 2007.

[34] M. Puchalski and A. Czarnecki. *Phys. Rev. Lett.*, **101**:183001, 2008.

[35] M. Puchalski, A. Czarnecki, and S. G. Karshenboim. *Phys. Rev. Lett.*, **99**:203401, 2007.

[36] T. K. Rebane and N. D. Markovskii. *Opt. Spec.*, **89**:667–671, 2000.

[37] Y. Suzuki and J. Usukura. *Nucl. Instr. and Math. in Phys. Res. B*, **171**:67–80, 2000.

[38] J. A. Wheeler. *Ann. N. Y. Acad. Sci.*, **48**:219, 1946.

# 7 Appendix - Alternate Approach to Three and Four-Body Integrals

In §4.3 and §5.3 we introduced coordinate shifts to help solve the integrals for the three and four-body matrix elements. Through suitable coordinate shifts the matrix elements could be transformed into easily integrable three-dimensional Gaussians since the wave functions themselves were Gaussians depending only upon the scalar interparticle distances. However, one is not always lucky enough to be using a trial wave function that can be simplified using this approach. Here we discuss another method for finding three and four-body matrix elements by breaking down the integration measure into one-dimensional interparticle scalar distances and angles. This method of integration has the advantage that one is always working to integrate over physical degrees of freedom of the system that can be visualized.

## 7.1 Three-body Integrals

In the lab frame where particles' positions are given by the vectors $\vec{A}_{1,2,3}$ the volume element that allows one to integrate over the positions of all particles is given by

$$\mathrm{d}V_3 \equiv \mathrm{d}^3\vec{A}_1\mathrm{d}^3\vec{A}_2\mathrm{d}^3\vec{A}_3.$$

In §4.3 we showed how one could move from the lab frame coordinates to relative coordinates $\vec{r}_{ij}$ (see Figure 5).

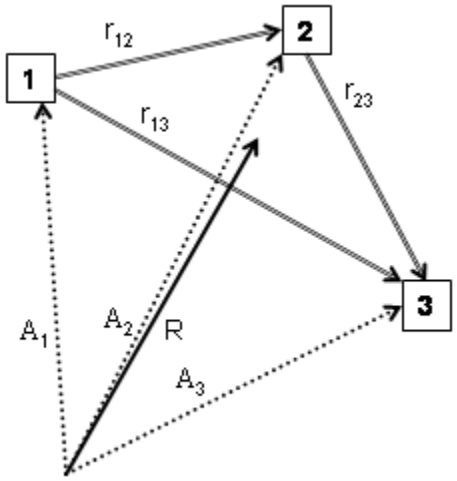


Figure 5: Three-body system in absolute coordinates $\vec{A}_i$ and relative coordinates $\vec{r}_{ij}$.

After making these coordinate changes the volume element becomes

$$\mathrm{d}V_3 = \mathrm{d}^3\vec{r}_{12}\mathrm{d}^3\vec{r}_{13}\mathrm{d}^3\vec{R} \equiv \mathrm{d}^3\vec{R}\mathrm{d}v_3.$$

We then argued that the term $\mathrm{d}^3\vec{R}$ which corresponded to the position of the centre-of-mass could be disregarded in the integration. Thus we are left with just $\mathrm{d}v_3$ which has six degrees of freedom to integrate over. However, we really only need to integrate over all possible configurations of the three particles. If we imagine the three particles

forming a triangle then the orientation of this triangle is not important. Since the orientation of this triangle requires three degrees of freedom we are actually only left with three degrees of freedom to cover all possible configurations of our system. This makes sense since the shape of a triangle is fixed given the knowledge of its three edge lengths.

In order to flush out the degrees of freedom associated with the orientation of the triangle let us the fix our triangle of particles in space so that particle $\{1\}$ is at the origin (see Figure 6).

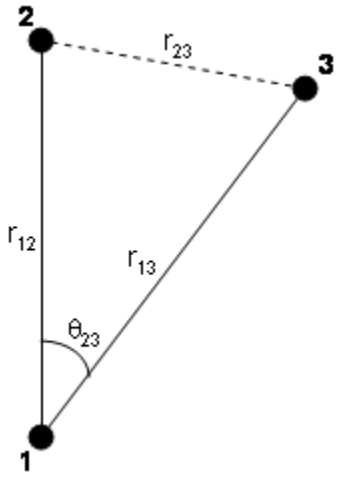


Figure 6: Fixing the orientation of the three-body system to remove orientational degrees of freedom in the volume element.

Next we will demand that particle $\{2\}$ lies on a fixed vertical axis. In doing so we will pick up a factor of $4\pi$ for the orientation of $\vec{r}_{12}$. Finally, let us fix $\vec{r}_{13}$ in a circle at an angle $\theta_{23}$ from $\vec{r}_{12}$. This contributes an additional factor of $2\pi$. Our volume element can then be written

$$\mathrm{d}^3\vec{r}_{12}\mathrm{d}^3\vec{r}_{13} = 8\pi^2 r_{12}^2 \mathrm{d}r_{12} r_{13}^2 \mathrm{d}r_{13} \mathrm{d}\cos\theta_{23}, \tag{181}$$

where $r_{12}, r_{13} \in (0, \infty)$ and $\theta_{23} \in (0, \pi)$. There are no more degrees of freedom that can be eliminated from the volume element, but it is useful to replace the integration over the angle $\theta_{23}$ by integration over the remaining scalar distance $r_{23}$. The law of cosines give us that

$$(\vec{r}_{12} - \vec{r}_{13})^2 \quad = \quad r_{23}^2 = r_{12}^2 + r_{13}^2 - 2r_{12}r_{13}\cos\theta_{23},$$

or

$$|r_{23}\mathrm{d}r_{23}| \quad = \quad |r_{12}r_{13}\mathrm{d}\cos\theta_{23}|\,.$$

The volume element (181) then becomes simply

$$\mathrm{d}^3\vec{r}_{12}\mathrm{d}^3\vec{r}_{13} = 8\pi^2 r_{12}\mathrm{d}r_{12}\, r_{13}\mathrm{d}r_{13}\, r_{23}\mathrm{d}r_{23}, \tag{182}$$

where $r_{12}$, $r_{13} \in (0, \infty)$ and $r_{23} \in (|r_{12} - r_{13}|, |r_{12} + r_{13}|)$. The bounds of integration for $r_{23}$ correspond to when $\vec{r}_{12}$ and $\vec{r}_{13}$ are anti-parallel and parallel respectively.

### 7.2 Four-body Integrals

Starting from the lab frame where the particles' positions are given by the vectors $\vec{A}_{1,2,3,4}$ we can write down the volume element that allows one to integrate over the positions of all particles as

$$\mathrm{d}V_3 \equiv \mathrm{d}^3\vec{A}_1 \mathrm{d}^3\vec{A}_2 \mathrm{d}^3\vec{A}_3 \mathrm{d}^3\vec{A}_4.$$

In §5.3 we showed how to change from absolute coordinates to relative coordinates $\vec{r}_{ij}$ (see Figure 7).

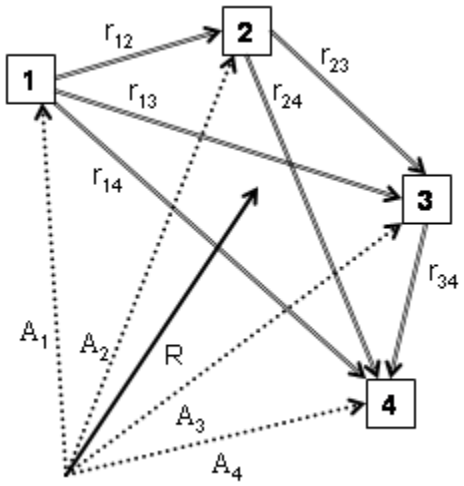


Figure 7: Four-body system in absolute coordinates $\vec{A}_i$ and relative coordinates $\vec{r}_{ij}$.

In doing so the volume element becomes

$$\mathrm{d}V_3 = \mathrm{d}^3\vec{r}_{12} \mathrm{d}^3\vec{r}_{13} \mathrm{d}^3\vec{r}_{14} \mathrm{d}^3\vec{R} \equiv \mathrm{d}^3\vec{R} \mathrm{d}v_3.$$

The term $\mathrm{d}^3\vec{R}$ corresponds to the position of the centre-of-mass so can be disregarded in the integration. Thus we are left with just $\mathrm{d}v_3$, which has nine degrees of freedom to integrate over. However, we only need to integrate over all possible configurations of the four particles. The four particles form a tetrahedron in space and the orientation of this tetrahedron is not important. Since the orientation is determined by three degrees of freedom, we are actually only left with six degrees of freedom to cover all possible configurations of our system. This makes sense since the shape of a tetrahedron is fixed if the lengths of its edges are known.

Let us remove the degrees of freedom associated with the orientation of the tetrahedron by first fixing it in space so that particle $\{1\}$ is at the origin (see Figure 8).

Next we will demand that particle $\{2\}$ lies on a fixed vertical axis. In doing so we will pick up a factor of $4\pi$ for the orientation of $\vec{r}_{12}$. We will then fix $\vec{r}_{13}$ in a circle at

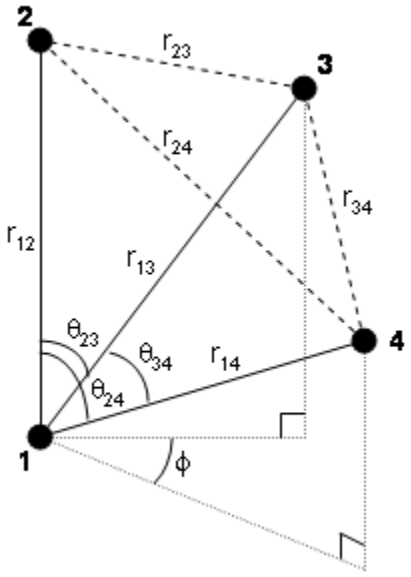


Figure 8: Fixing the orientation of the four-body system to remove orientational degrees of freedom in the volume element.

an angle $\theta_{23}$ from $\vec{r}_{12}$. This contributes an additional factor of $2\pi$. The final vector $\vec{r}_{14}$ is free to point in any direction and still give rise to a unique configuration so no degrees of freedom can be eliminated here. Now, let us break up the integration over $\vec{r}_{14}$ into integration over the scalar distance $r_{14}$, the angle between $\vec{r}_{12}$ and $\vec{r}_{14}$ which we will call $\theta_{24}$, and the angle between the triangle formed by particles $\{1,2,3\}$ and $\{1,2,4\}$ which we will denote by $\phi$. Our volume element can then be written

$$\mathrm{d}^3\vec{r}_{12}\mathrm{d}^3\vec{r}_{13} = 8\pi^2 r_{12}^2 \mathrm{d}r_{12} r_{13}^2 \mathrm{d}r_{13} r_{14}^2 \mathrm{d}r_{14} \mathrm{d}\cos\theta_{23} \mathrm{d}\cos\theta_{24} \mathrm{d}\phi, \tag{183}$$

where $r_{12}$, $r_{13}$, $r_{14} \in (0,\infty)$, $\theta_{23}$, $\theta_{24} \in (0,\pi)$, and $\phi \in (0,2\pi)$. Using the law of cosines one can attempt to write the volume element purely in terms of scalar distances. However, a more convenient form is given in [32] using the angle between $\vec{r}_{13}$ and $\vec{r}_{14}$ (denoted $\theta_{34}$) instead of the angle $\phi$. In this case the volume element (183) becomes

$$\mathrm{d}^3\vec{r}_{12}\mathrm{d}^3\vec{r}_{13}\mathrm{d}^3\vec{r}_{14} \propto \frac{r_{12}^2 \mathrm{d}r_{12} r_{13}^2 \mathrm{d}r_{13} r_{23}^2 \mathrm{d}r_{23} \mathrm{d}\cos\theta_{23} \mathrm{d}\cos\theta_{24} \mathrm{d}\cos\theta_{34}}{\sqrt{1-\cos^2\theta_{23}-\cos^2\theta_{24}-\cos^2\theta_{34}+2\cos\theta_{23}\cos\theta_{24}\cos\theta_{34}}}. \tag{184}$$

With this volume element, the bounds of integrations on the distances are still $r_{12}$, $r_{13}$, $r_{14} \in (0,\infty)$, but the angles are not independent. In particular, if we choose to integrate $\theta_{23}$, $\theta_{24} \in (0,\pi)$, then the remaining angle only spans the range $\theta_{34} \in (|\theta_{23}-\theta_{24}|, |\theta_{23}+\theta_{24}|)$. The minimum corresponding to when the triangles formed by particles $\{1,2,3\}$ and $\{1,2,4\}$ are overlapping in the same plane and the maximum to when the triangles are in the same plane not overlapping (see Figure 9).

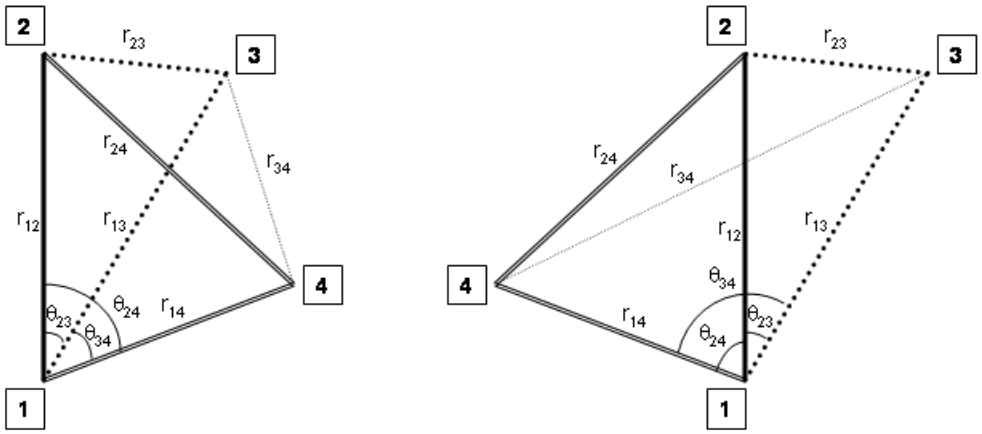


Figure 9: Given values for two angles, say $\theta_{23}$ and $\theta_{24}$, the third angle ranges from $\theta_{34} = |\theta_{23} - \theta_{24}|$ (left) to $\theta_{34} = |\theta_{23} + \theta_{24}|$ (right).

### 7.3 Example for Three-body Overlap Integral

To demonstrate the equivalence of the different integration methods let us consider the overlap integral for the three-body problem in §4.3. With the trial wave function

$$|\psi_i\rangle = \exp\left\{-a_i r_{12}^2 - b_i r_{13}^2 - d_i r_{23}^2\right\}, \tag{185}$$

one aims to solve the integral

$$I(a,b,d) = \int \mathrm{d}^3\vec{r}_{12}\mathrm{d}^3\vec{r}_{13}\, e^{-ar_{12}^2 - br_{13}^2 - dr_{23}^2}. \tag{186}$$

Using the volume element (182) gives

$$\begin{aligned} I(a,b,d) &= 8\pi^2 \int_0^\infty r_{12}\mathrm{d}r_{12} \int_0^\infty r_{13}\mathrm{d}r_{13} \int_{|r_{12}-r_{13}|}^{|r_{12}+r_{13}|} r_{23}\mathrm{d}r_{23} \\ &\quad \times e^{-ar_{12}^2 - br_{13}^2 - dr_{23}^2} \\ &= \frac{-4\pi^2}{d} \int_0^\infty r_{12}\mathrm{d}r_{12} \int_0^\infty r_{13}\mathrm{d}r_{13} \\ &\quad \times \left[e^{-er_{12}^2 - fr_{13}^2 - 2dr_{12}r_{13}} - e^{-er_{12}^2 - fr_{13}^2 + 2dr_{12}r_{13}}\right], \end{aligned}$$

where $e \equiv a + d$ and $f \equiv b + d$. Next let $u \equiv \sqrt{e}r_{12}$ and $v \equiv \sqrt{f}r_{13}$ then

$$\begin{aligned} I(a,b,d) &= \frac{-4\pi^2}{def} \int_0^\infty u\,\mathrm{d}u \int_0^\infty v\,\mathrm{d}v \\ &\quad \times \left[e^{-u^2 - v^2 - 2guv} - e^{-u^2 - v^2 + 2guv}\right], \end{aligned}$$

with $g = \frac{d}{\sqrt{ef}}$. Using a suitable coordinate change we can eliminate the cross-term in the exponentials. So let $x \equiv u \pm gv$ and $y \equiv \sqrt{1-g^2}v$. The Jacobian for this transformation is just $\frac{\partial(x,y)}{\partial(u,v)} = \sqrt{1-g^2}$. The integral then becomes

$$
\begin{aligned}
I\left(a,b,d\right) &= \frac{-4\pi^2}{def\left(1-g^2\right)}\int_0^\infty \mathrm{d}y\, y\, e^{-y^2} \\
&\quad \times\left[\int_{gy}^\infty \mathrm{d}x\left(x-\frac{gy}{\sqrt{1-g^2}}\right)e^{-x^2}\right. \\
&\quad \left.-\int_{-gy}^\infty \mathrm{d}x\left(x+\frac{gy}{\sqrt{1-g^2}}\right)e^{-x^2}\right] \\
&= \frac{8\pi^2 g}{def\left(1-g^2\right)^{3/2}}\left(\int_0^\infty \mathrm{d}y\, e^{-y^2}\right)\left(\int_0^\infty \mathrm{d}x\, x^2\, e^{-x^2}\right) \\
&= \frac{\pi^3 g}{def\left(1-g^2\right)^{3/2}} \\
&= \frac{\pi^3}{\left(ef-d^2\right)^{3/2}} \\
&= \frac{\pi^3}{\left(ab+ad+bd\right)^{3/2}}.
\end{aligned}
$$

This result is identical to equation (61) as should be expected. It is clear that this method is much more cumbersome for this integral than that used in §4.3, however, we present this alternative approach because for other choices of trial wave functions or the expectation values of certain operators the opposite may be true.

# 8 Appendix - Perturbative Matching for Effective Field Theory Coefficients

In §4.1 and §5.1 we constructed effective field theories by modifying the Coulomb potential to remove the divergence. We then introduced a series of operators to reproduce the local interactions. These operators were defined in terms of a function $\delta_\Lambda^3(r)$ and an infinite set of parameters $d_i$. Given a particular choice for the function $\delta_\Lambda^3(r)$, the parameters $d_i$ would then be determined uniquely if we wanted to reproduce the true theory entirely. That is, if we wanted

$$V(r) = \frac{1}{r}$$

equal to

$$V^\Lambda(r) = \frac{1}{r}\text{erf}\left(\frac{\Lambda r}{\sqrt{2}}\right) + \frac{d_1}{\alpha^2}\delta_\Lambda^3(r) - d_2\nabla_r^2\delta_\Lambda^3(r) + d_3\nabla_r\delta_\Lambda^3(r)\cdot\nabla_r....$$

Determining all of the parameters is a hopeless task. Fortunately, it turns out that if we only want our effective theory to be valid to a given accuracy then only a finite number of correction terms are needed. For our purposes, we only required agreement through $\mathcal{O}(\alpha^3)$. This meant we only needed $d_1^{(1)}$ and $d_1^{(2)}$, where $d_1$ had been expanded in $\alpha$ (i.e. $d_1 = \alpha d_1^{(1)} + \alpha^2 d_1^{(2)} + ...$). To see why this is let us write down our true and effective potentials in momentum space. The Coulomb potential is simply

$$V(q) = \frac{4\pi}{q^2}, \tag{187}$$

while the effective potential without corrections is

$$V^\Lambda(q) = \frac{4\pi}{q^2}\exp\left\{-\frac{q^2}{2\Lambda^2}\right\}, \tag{188}$$

and the local operator generating function will become

$$\delta_\Lambda^3(q) = \alpha^3\exp\left(-\frac{q^2}{2\Lambda^2}\right).$$

The correction terms then give a series in momenta squared,

$$C^\Lambda(q) = \left(\frac{d_1}{\alpha^2} + d_2q^2 + d_3\vec{l}\cdot\vec{k} + \mathcal{O}(q^4)\right)\delta_\Lambda^3(q). \tag{189}$$

The coefficients $d_i$ can be determined via perturbative matching. For example, at lowest order, we have the scattering amplitude from the effective theory as

$$\begin{aligned} T_{eff}^{(1)}\left(\vec{l}\to\vec{k}\right) &= \left[\frac{4\pi}{q^2} + \alpha d_1 + \alpha^3 d_2 q^2 + \alpha^3 d_3\vec{l}\cdot\vec{k} + ...\right]\exp\left(-\frac{q^2}{2\Lambda^2}\right) \\ &= \frac{4\pi}{q^2} + \left(\alpha d_1 - \frac{2\pi}{\Lambda^2}\right) + \left(\alpha^3 d_2 - \frac{d_1\alpha}{2\Lambda^2} + \frac{\pi}{2\Lambda^4}\right)q^2 \\ &\quad + \alpha^3 d_3\vec{l}\cdot\vec{k} + \mathcal{O}(q^4) \end{aligned} \tag{190}$$

The Born approximation gives the $\mathcal{O}(\alpha)$ result $T^{(1)}_{exact} = \frac{4\pi}{q^2}$. Expanding the parameters $d_i = \alpha d_i^{(1)} + \alpha^2 d_i^{(2)} + ...$ and demanding that the two methods give the same result at $\mathcal{O}(\alpha)$ for all $q$, equation (190) then tells us that:

$$d_1^{(1)} = \frac{2\pi}{\alpha^2 \Lambda^2},$$

$$d_2^{(1)} = \frac{\pi}{2\alpha^4 \Lambda^4},$$

$$d_3^{(1)} = 0.$$

At the next order, we can compare the threshold scattering amplitudes and demand

$$\lim_{\vec{k} \to 0} \left[ T^{(2)}_{eff}\left(\vec{l} \to \vec{k}\right) - T^{(2)}_{exact}\left(\vec{l} \to \vec{k}\right) \right] = 0,$$

If one does this they will find

$$\begin{aligned} d_1^{(2)} &= \sqrt{\pi}\left[ \frac{10}{3\alpha^3\Lambda^3} + 20\alpha\Lambda \frac{d_2^{(1)}}{4\pi} - 6\alpha^5\Lambda^5 \left( \frac{d_2^{(1)}}{4\pi} \right)^2 \right] \\ &= \frac{71\sqrt{\pi}}{96\alpha^3\Lambda^3}, \end{aligned}$$

which completes the correction at one-loop order. This procedure can be repeated to determine coefficients that give agreement between the exact and effective theories to any desired accuracy. For our investigation, we required energy levels accurate only through $\mathcal{O}\left(\alpha^3\right)$ (in energy units $m\alpha^2$) so we could set $d_2^{(i)} = 0$ for all $i$. This then gives the only non-zero coefficients as

$$d_1^{(1)} = \frac{2\pi}{\alpha^2 \Lambda^2},$$

$$d_1^{(2)} = \frac{10\sqrt{\pi}}{3\alpha^3\Lambda^3},$$

in agreement with those of §4.1 and §5.1.

# 9 Appendix - Computer Software

In this section we discuss the details of the program used to solve the generalized eigenvalue problem and implement Powell's method to minimize the result. This program requires the input of a pair of functions to generate the Hamiltonian and overlap matrix elements given a set of parameters. Once the matrix elements are computed the eigenvalue problem is solved. The program then repeats this process while varying the parameters so that it can seek out optimal values for these parameters and minimize the result from solving the eigenvalue problem. Upon completion the program outputs the minimized energy and the parameters that produce it as well as the corresponding eigenvector. From the parameters and eigenvector one can construct the wave function and compute expectation values. The program uses double precision and runs on a single processor.

## Program Files

The files used by this program can be broken up into two groups - those written by the author and those from Numerical Recipes [33]. The files written by the author include:

**main.cpp** This is the control centre for the program. From this file the parameters are passed around to various functions to be tuned and compute quantities of interest. This is also where one specifies what external files to include, what values to choose for global constants, and how the output should be handled.

**tools.h** This is where all custom written functions are stored. In particular it includes a function for performing QR decomposition, a function for solving the generalized eigenvalue problem, a function for updating a QR decomposition, and many other minor functions which perform matrix operations and debugging. All matrix operations required are custom written into this file or part of the Numerical Recipes routine so as to exclude the overhead that comes with using a linear algebra package.

**outcom.h** This file includes functions which handle input from and output to files. In particular, input and output of tuned energies, eigenvectors, and parameter sets.

**psion.h/ps2.h** This is where the functions for computing matrix elements and expectation values for a particular physical system are stored.

The operations handled with Numerical Recipes code in this program are Powell's method, QR decomposition, and QR decomposition update. The files containing these routines along with all other files supporting the use of these three are:

**powell.cpp** Runs the Powell routine. Accepts input of a set of parameters, a directional matrix for the minimization process, an error tolerance, and a function of the parameters to minimize. For the problems at hand the function to minimize called **func** is the custom routine (found in **tools.h**) which solves the generalized eigenvalue problem.

**linmin.cpp** Called by **powell.cpp**. Finds the minimum of a function in a particular direction in multidimensions.

**mnbrak.cpp** Called by **linmin.cpp**. Brackets a minimum.

**brent.cpp** Called by **linmin.cpp**. Uses Brent's method to seek out a minimum.

**f1dim.cpp** Constructor called by **linmin.cpp** for evaluating a function efficiently.

**qrdcmp.cpp** Performs a QR decomposition of an input matrix. Output is in the form of two vectors from which one must construct the $Q$ and $R$ matrices (see function **upperTri2** in **tools.h** for details).

**qrupdt.cpp** Updates a QR decomposition based on the input of two vectors whose outer product gives the change in the product of the $Q$ and $R$ matrices.

**rotate.cpp** Routine called by **qrupdt.cpp**.

Also needed to run the Numerical Recipes routines is the header file **nr.h**. If you change the arguments of a Numerical Recipes routine then you must also change its definition in **nr.h**. More details on the Numerical Recipes code can be found in [33].

### Overview of Program

We now give a more thorough discussion of the custom written files: **main.cpp**, **tools.h**, **outcom.h**, and **psion.h**/**ps2.h**.

**main.cpp**

At the beginning of the file **main.cpp** one finds an assortment of global constants. The purpose of each constant is as follows:

- **DP FTOL** - Specifies the acceptable error tolerance for the Powell routine and so determines to what precision the parameters are tuned.
- **DP LINTOL** - Specifies the acceptable error tolerance for the linmin routine.
- **DP ETOL** - Specifies the acceptable error tolerance when calculating the change in energy in function **func** (see **tools.h**).
- **DP ENERGY** - Starting estimate for energy of system, should be close to actual energy otherwise inverse iteration can run into problems.
- **int NPAR** - Number of parameters per wave function (e.g. 3 for positronium-ion, 6 for di-positronium).
- **int SubSteps** - Number of times to run a full QR decomposition to update the energy and eigenvector each time the Hamiltonian and Overlap matrices are recomputed from scratch.
- **int SubSteps2** - Maximum number of times to test a set of parameters in **func** (see **tools.h**) within the Powell routine when trying to calculate the change in energy for those parameters. If the change in energy is deemed acceptable then this loop is broken but occasionally multiple iterations are needed to find an eigenvector that gives a good change in energy.
- **int MAXITS** - Number of times the Powell routine cycles through the full set of parameters.

- **int CYCLESTEPS** - The number of times you wish to grow the basis. At the end of each **CYCLESTEP** you must increase **CYCLE**.
- **int NDIM** - The total number of basis functions to use in the optimization process. This number should be equal to **CYCLE** if you do not grow the basis. If you do plan to grow the basis size then this should be the final basis size, larger than **CYCLE**.
- **int RESETMAX** - Number of times to use **funcQRupdate** (refer to **tools.h**) before performing a full QR decomposition to eliminate accumulated errors. QR decompositions take time $\mathcal{O}\left(N^3\right)$ while updates take $\mathcal{O}\left(N^2\right)$. For small basis sizes it is alright to have smaller **RESETMAX** because the decompositions do not take too long and they allow you to improve your eigenenergy and eigenvector faster. However, as the basis size gets bigger it is inefficient to calculate the full decomposition often so **RESETMAX** should be increased, but not so large that errors spoil results.
- **DP CUTOFF** - This is the momentum cutoff from the effective field theory, this term only shows up in **psion.h** and **ps2.h**. It is in units $m\alpha$ here.
- **int CYCLE** - The current basis size that you are working in. At the end of each loop of **CYCLESTEP** you must give some prescription for how **CYCLE** grows.
- **int RESET** - A counter to keep track of how many times we have done a QR update without having done a full QR decomposition.

Immediately following these definitions there are a series of strings which reference input and output files. If you are concerned with input and output then these must be changed constantly.

We are now ready to look at the contents of the **main** function. At the beginning of the **main** function we define all of our working variables, vectors, and matrices (e.g. parameter set, Hamiltonian matrix, overlap matrix, eigenvector). We then initialize the parameters so that each parameter is a function of some random number (see **initParams** in **tools.h**). This function is chosen so that the resulting parameters are roughly the right order of magnitude for the positronium-ion and di-positronium molecule. Next, we initialize our eigenvector to be normalized with all equal entries (this will soon change). The last step before parameter optimization is to read in any external data if desired. This is done with the functions in **outcom.h** such as **readAll**.

The first loop that we enter in starting the optimization runs for a total of **CYCLESTEPS** times. As discussed above, each iteration of this loop deals with a certain basis size. Thus at the beginning of this loop we must compute the Hamiltonian and overlap matrices and renormalize the eigenvector. At this point we must also perform a full QR decomposition because the basis size has changed. This also updates the eigenvector and energy.

The next loop with loop variable maximum **MAXITS** determines how many times we will run through the entire basis in our optimization. For larger basis sizes this loop need not run many times because the tuning of the new parameters will be relatively independent of the other pretuned ones. As an alternative to having a loop

that runs a definite number of times one may also define a termination condition depending on how much the energy changes between each step. That is, if we run this loop and the energy does not decrease by a minimum amount then we break and grow the basis.

The last loop in the nest is where the actual optimization takes place. For each cycle of the loop we run through the parameters of each trial wave function once. We work with all of the parameters for a particular wave function at once and store them in a temporary vector **p**. We then run the Powell routine with this vector as the argument of the function **func** which is to be minimized (see below for more details on **func**). The Powell routine should return a set of parameters that reduce the upper bound on the energy and, if so, we overwrite the current parameters for the wave function being worked on with these new ones. Before we move on, we compute the updated QR decomposition for the new parameters (see **funcQRupdate** below). Additionally, if we have updated the QR decomposition **RESETMAX** times then we recalculate the Hamiltonian and overlap matrices from scratch and recompute the full QR decomposition to remove errors. At this point the optimization of the parameters of a single wave function is finished and we reset the counter **iter** for the Powell routine.

Once we have finished optimizing at a particular basis size (finished the two inner loops) we will have a set of tuned parameters, a tuned eigenvector, and a minimized energy. We can use the parameters and eigenvector to reconstruct a full wave function which can then be used to work out expectation values for this basis size. Finally, we write our results to a file and increment **CYCLE** to grow the basis.

**tools.h**

In **tools.h** are all of the custom written functions which primarily deal with the linear algebra aspects of the problem. The following is a list of the functions along with their purposes:

**multMat** Performs simple matrix multiplication.

**multMatVec** Multiplies a matrix and a vector.

**dispMat** Outputs a matrix to the console (primarily used for debugging).

**dispVec** Outputs a vector to the console.

**initParamsRand** Creates a set of random parameters.

**initIdent** Creates an identity matrix.

**equalMat** Sets a matrix equal to another one.

**transpose** Finds the transpose of a matrix.

**norm** This function is overloaded and can perform three operations. If one inputs a vector and a float then it will return the vector unchanged but return the norm of the vector as the float. If one inputs just a vector the function will return it normalized. Finally, if one inputs two vectors and a float it will return the norm of the difference of the two vectors as the float.

**upperTri2** Finds the QR decomposition of an input matrix using the Numerical Recipes routine **qrdcmp.cpp**. Returns the R matrix in place of the matrix input to be decomposed and Q in place of an input dummy matrix.

**combineMat** Outputs a linear combination of two matrices.

**QRBackSub** Solves the matrix equation $R\vec{y} = \vec{x}$ for $\vec{y}$ where $\vec{x}$ and $R$ are given with $R$ being an upper triangular matrix.

**QRIIDecomp** This function is designed to take a Hamiltonian matrix, $H$, an overlap matrix, $W$, a trial energy, $E$, and a trial eigenvector $\psi$ and return the QR decomposition of $(H - EW)$. It then uses inverse iteration to update the energy and find an eigenvector of $H$ corresponding to the eigenenergy $E$. It accomplishes this by using the QR decomposition and back substitution to solve the equation $(H - EW)\,\psi' = QR\psi' = W\psi$ for $\psi'$. Inverse iteration theory tells us that $\psi'$ will be closer to the true eigenvector of $H$ corresponding to the eigenvalue $E$ than $\psi$ was. We can then use this new eigenvector along with the old one to update the energy according to $E' = E + \frac{\psi' \cdot W \cdot \psi}{\psi' \cdot W \cdot \psi'}$.

**func** This is the function that the Powell routine minimizes. It accepts the set of parameters currently being tuned as well as the full parameter set, the Hamiltonian matrix, the overlap matrix, the full QR decomposition, the current energy, and the current eigenvector. Using the Numerical Recipes routine **qrupdt.cpp** we can find the new $Q$ and $R$ matrices as if our full parameter set included the parameters currently being tuned instead. Using the updated QR decomposition we can solve the equation $(H - EW)\,\psi' = W\psi$ for a new eigenvector $\psi'$ given our current eigenvector $\psi$. The new eigenvector can then be used to calculate the new energy as a result of using the trial parameters being tuned in our full parameter set. However, this method is not infallible so we calculate the energy change in two ways: (1) $\Delta E_1 = \frac{\psi' \cdot W \cdot \psi}{\psi' \cdot W \cdot \psi'}$ as in **QRIIDecomp** and (2) $\Delta E_2 = \frac{\psi \cdot W \cdot \psi}{\psi \cdot W \cdot \psi'}$. If our new eigenvector improves then these two energies should agree. If this is the case then we break and return this change in energy. However, occasionally the updating method fails and one cannot find a good eigenvector so we can repeat this process until either we find one or reach some maximum number of iterations. If the latter happens then we return a small positive quantity for $\Delta E$ so that Powell knows that these parameters will not help minimize the energy. It is important to note that this function does not change anything permanently. It only temporarily overwrites elements of the full parameter set to test them.

**funcQRupdate** This function updates the QR decomposition as well as the Hamiltonian and overlap matrices using the newly tuned parameters resulting after each execution of the Powell routine. It does this by using the Numerical Recipes routine **qrudpt.cpp**. We do not update the energy here because then the QR decomposition $QR = (H - EW)$ would then no longer be valid. It is important to note that since this function only updates matrices it allows for the accumulation of error. To prevent this error from building up to the point where it spoils the calculations it is important to occasionally recompute the Hamiltonian and overlap matrices from scratch and then run QRIIDecomp.

**outcom.h**

In this file we store all of the functions that deal with input to and output from files. The most notable functions are:

- **writeAll** which outputs the current basis size, energy, parameter set, and eigenvector. Using these values one can restart the program where it left off and also construct the full wave function for the purpose of calculating expectation values and,
- **readAll** which reads in a basis size, energy, parameter set, and eigenvector. Using this we can take the data from a file created by **writeAll** and pick up where we left off in a previous program.

**psion.h/ps2.h**

These files contain all of the functions specific to the physical problem at hand. In other words, if you replace this file with another one that had a similar set of functions you could use the program to solve that system (you may also need to change the global constants **NPAR** and **ENERGY**). Obviously, this means that if we include the file **psion.h** we will be working with the positronium-ion and if we include **ps2.h** we will be working with the di-positronium molecule. Only one of these files should be included for a particular run.

Inside these files you will find all of the functions which generate the matrix elements for the corresponding physical system's Hamiltonian, overlap matrix, and expectation values. For example, upon opening either file one finds a set of functions **overlap**, **kin_part**, **exact_pot_part**, **cutoff_part**, etc. These functions are used to generate the matrix elements worked out in §4.3 (positronium-ion) or §5.3 (di-positronium molecule) before taking into account the symmetries of the system. In particular, the **overlap** function works out a matrix element in the overlap matrix, the **kin_part** function work out the kinetic energy part of a matrix element of the Hamiltonian matrix, and so on. These functions are then called by the functions **prepareH** and **prepareW** which calculate the matrix elements individually to construct the entire Hamiltonian and overlap matrices. On top of this they also take into account the symmetries of the system by calling the matrix element functions multiple times for different ordering of the parameters and then adding together each result. If one only needs to calculate a single element of the Hamiltonian or overlap matrix then you can use **Helem** or **Welem** respectively. **IMPORTANT** - the functions **prepareH** and **Helem** are where one can choose if the program is going to work with the exact potential or the cutoff potential. This is accomplished by uncommenting the definition of **hmat** at the end of these functions corresponding to your choice. After this, these files include various functions for computing expectation values of various operators.

## Compiling and Executing the Program

### UNIX

In the Unix environment we use the GNU compiler for C++ to build the program. To compile, enter at the command line from the directory of the **main.cpp** file

***g++ main.cpp -o mainprog***

The part ***g++ main.cpp*** tells the compiler to compile the source code in the file **main.cpp**. The next part ***-o mainprog*** directs the output (which will be an executable) into a file named **mainprog**.

We are now ready to run the program. To do this one can enter at the command line simply

***./mainprog***

However, since these programs typically take a long time and one would like to work on other things while the program is running it is more useful to use

***nice - n 10 nohup ./mainprog > outfile.dat &***

The command ***nice -n 10*** lowers the priority of the program so that other users can run short programs on the same processor and be able to use the majority of the processor's speed. The command ***nohup*** tells the program to continue running even if you log out. The ampersand tells the program to run in the background and ***> outfile.dat*** tells the program to output data that would normally show up in the console to instead be saved in a file named **outfile.dat**. If this file does not exist then it will be created automatically.

### Windows

The software Dev-C++ by BloodshedSoftware (www.bloodshed.net) is highly recommended when working in Windows. This software allows you to compile and run the code with the click of a button.